M.A. Oort

The existence of bilayer structures of amphiphilic polymers through the multi-component functionalized Cahn-Hilliard free energy

Master's Thesis, September 29, 2016

Thesis Adviser: prof.Dr. A. Doelman

Mathematisch Instituut, Universiteit Leiden

Abstract

In this master's thesis, we consider a model for the free energy of two amphiphilic polymers in a bulk solvent. We are interested in the minimizers of this model, representing the most energetically favorable configurations, and specifically study the existence of lipid bilayers, which partition the solvent phase as a co-dimension one subspace. To find such bilayers, we will look for a stationary pulse solution of a system of partial differential equations describing the volume fractions of the polymers over time. We will use geometric singular perturbation theory as posed by Neil Fenichel, and follow techniques used in earlier work on similar systems of differential equations. We will see that the system admits a stationary pulse solution for a flat bilayer, but that introducing a curvature of the bilayer to the system eliminates the possibility of such a solution.

Contents

1 Biochemical and Mathematical Background

1.1 Amphiphilic Polymers

A molecule or substance is called *amphiphilic* if it has favorable energetic interactions at the interface of two fluids. A well-known example of such an amphiphilic substance is soap in oily water, where the soap possesses both hydrophilic (water-loving) and lipophilic (fat-loving) properties, and is thus able to separate the two. Traditionally, the fluids involved had to be essentially different but due to developments in synthetic chemistry it has become more easily possible to create amphiphilic polymers. Polymers are very large molecules composed of many repeated subunits and it is possible through atom transfer radical polymerization to add a hydrophilic group to a hydrophobic (water-fearing) polymer, creating a polymer that does not have favorable energetic interactions with multiple distinct fluids, but now has both favorable and unfavorable interactions with the solvent they are in. This is what we mean with amphiphilic polymers.

Thus, when we mix amphiphilic polymers with a solvent the polymers try to form formations that are energetically the most favorable, for which a few possibilities arise. Which one of these possible formations arises depends on many different factors, such as solvent type, pH and temperature.

The polymers can form a structure that partitions the solvent phase by so-called *lipid bilayers*, where the hydrophilic parts of the polymers are exposed to the solvent and the hydrophobic parts are secluded within the bilayer (Figure 1, left). As this bilayer is a two-dimensional figure in three-dimensional space, we say it has *co-dimension* one (the co-dimension of a subspace is the difference between the dimension of the subspace and the space itself).

The polymers can also form a lipid pore, which is a string that also has the hydrophilic parts facing to the solvent and hydrophopic parts separated, but does not partition the solvent (Figure 1, center). Thus, as this string is a one-dimensional subspace, the lipid pores are co-dimension two figures.

Lastly, the polymers can form micelles which are spherical forms with all hydrophobic parts facing each other (Figure 1, right). These micelles can be seen as points in three-dimensional space, meaning they have co-dimension three.

The lipid bilayer and lipid pore formations (Figure 1, left and center) are often collectively referred to as networks because they form a network morphology which self-assembles at the nano-scale, and these networks are interesting because they are often charge-selective. This makes them effective as selective ionic conductors, which are used in various types of energy conversion devices such as fuel cells, solar cells and ion batteries. Because of the possible applications of networks there has been some interest in the conditions for which

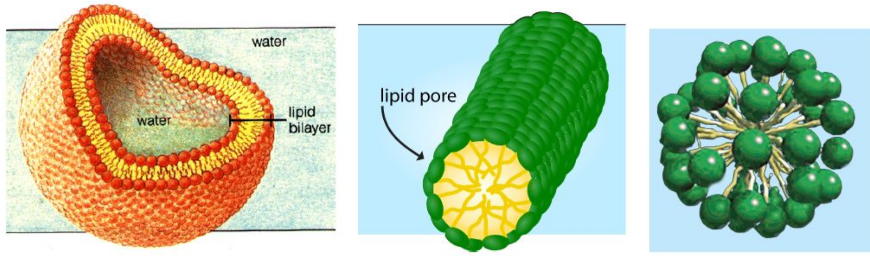

Figure 1: *Schematic of possible configurations of amphiphilic polymers in a solvent: a lipid bilayer (left), a lipid pore (center) and a micelle (right). The co-dimensions are respectively one, two and three.*

networks form and break up, and a lot has been studied experimentally. Bifurcations in the morphology of the polymers are observed by for instance by varying temperatures or by varying the length of the hydrophobic portions.[7]

Aside from the experimentally observations, it is also possible to model aforementioned bifurcations mathematically, using the 'functionalized Cahn-Hilliard (FCH) Free Energy'. This free energy models the interfacial energy in amphiphilic phase-separated mixtures meaning that the minimizers of the FCH are energetically the most favorable. Hence, the FCH may give us tools to find out which polymer formation is most favorable under certain conditions and whether this formation is stable or unstable.

This thesis will focus on an extension of the functionalized Cahn-Hilliard Free Energy to multiple components, which lets us model the free energy of two distinct polymers in a bulk solvent. But before introducing this multivariate model I will introduce the functionalized Cahn-Hilliard Free Energy as it was originally constructed, in the one component form. This will clarify the biological relevance of the model and makes it possible to show some simple examples and explanations, before going deeper into the thesis equations.

1.2 The functionalized Cahn-Hilliard Free Energy

Driven by data from small-angle X-ray scattering (SAXS) of micro-emulsions of soapy-oil within water, Tubner and Stray and later Gommper and Shick devised a model for the free energy for the soapy-oil fraction $u \in H^2(\Omega)$ of the following form: [8]

$$\mathcal{F}_{GS}(u) = \int_\Omega \varepsilon^4 \frac{1}{2} \|\Delta u\|^2 + \varepsilon^2 G_1(u) \Delta u + G_2(u)\, \mathrm{d}x.$$

Here $\Omega \subset \mathbb{R}^d$ is a fixed domain and $0 < \varepsilon \ll 1$ is used to denote the thickness of the interface involved. It must be noted that for the biological background described above, a choice of $d = 3$ would seem the most useful, but for generality we will just assume that $d \geq 2$ in this thesis.

The functionalized Cahn-Hilliard Free Energy is a simple case of this very general free energy model, where we choose $G_1 = -W'(u)$ and $G_2 = \frac{1}{2}(W'(u))^2 - \varepsilon^p P(u)$. The function $W : \mathbb{R} \to \mathbb{R}$ is assumed to be a double-well potential with two, typically unequal minima $u = u_\pm$. When we substitute these expressions for G_1 and G_2 into the Gompper and Schick free energy, and a specific choice for the potential P, we get the *functionalized Cahn-Hilliard Free Energy*:

$$\mathcal{F}_{CH}(u) := \int_\Omega \frac{1}{2}\left(\varepsilon^2 \Delta u - W'(u)\right)^2 - \varepsilon^p \left(\eta_1 \frac{\varepsilon^2}{2}|\nabla u|^2 + \eta_2 W(u)\right) \mathrm{d}x. \tag{1.1}$$

For this thesis, I will assume that the FCH correctly models the free energy for an amphiphilic polymer in a solvent, where $u \in H^2(\Omega)$ now denotes the volume fraction of the polymer. The rightmost term of (1.1) represents the functionalization, with functionalization parameters η_1 and η_2, and this term is very small in comparison with the left term because of multiplication with ε^p. Typical choices for p are $p = 1$ or $p = 2$, where the former is referred to as the *strong functionalization* and the latter as the *weak functionalization*. In this thesis I will focus only on the strong functionalization, where the bifurcation structure depends primarily on the bifurcation parameters. The biological interpretation of these parameters is that $\eta_1 \geq 0$ denotes the strength of the hydrophilic part of the functionalized polymer, and that $\eta_2 \in \mathbb{R}$ models pressure differences between the majority and minority phase. These pressure differences can arise for instance due to a crowding of hydrophobic tail groups in the hydrophobic domain, which happens in the case of lipids.[2]

We are interested in minimizing the energy and thus in finding minimizers of the FCH. Due to the ε^p term in front of the functionalization terms, the squared term on the left side of the FCH is dominant and hence, under zero-net flux boundary conditions, the minimizers of the FCH must make this term small as well. Thus these minimizers are close to solutions of

$$\varepsilon^2 \Delta u - W'(u) = 0, \tag{1.2}$$

which is an exact solution in the case that $\eta_1 = \eta_2 = 0$. Biologically this would mean that the hydrophilic part of the functionalized polymer has zero strength, and there is no pressure difference between the different phases, implying the polymer is not functionalized in the first place. This can also be seen from the fact that the solutions of equation (1.2) are precisely the critical points of the usual Cahn-Hilliard free energy

$$\mathcal{E}(u) := \int_\Omega \frac{\varepsilon^2}{2}|\nabla u|^2 + W'(u)\,\mathrm{d}x,$$

because $\mathcal{E}_u(u)$ equals the left side of (1.2).

Minimizing equation (1.1) corresponds to solving the gradient flow for the free energy, where we can choose from a broad class of admissible gradient $\mathcal{G}$. The exact requirements for admissibility of a gradient are given in [2], but the most important assumption is that the kernel of $\mathcal{G}$ is spanned by constant functions, i.e. $\ker(\mathcal{G}) = \{1\}$. This kernel guarantees that the evolution equation of the FCH

$$u_t = -\mathcal{G}\frac{\partial \mathcal{F}_{CH}}{\partial u},$$

is mass-preserving when subject to zero-flux boundary conditions. In [2], some typical choices for this $\mathcal{G}$ are explained. For either of these choices, the critical points of the FCH are solutions of the following equation

$$\frac{\partial \mathcal{F}_{CH}}{\partial u} := (\varepsilon^2\Delta - W''(u))(\varepsilon^2\Delta u - W'(u)) - \varepsilon^p(-\varepsilon^2\eta_1\Delta u + \eta_2 W'(u)) = \varepsilon\mu, \quad (1.3)$$

where μ is a free constant that spans the kernel of $\mathcal{G}$. This is a fourth order differential equation, and in [2], the authors show the existence of a homoclinic orbit to one of the zeroes of the potential $W(u)$. In equation (1.3) we can recognize again the expression $\varepsilon^2\Delta u - W'(u)$ and thus solutions of (1.3) are $\mathcal{O}(\varepsilon)$ close to solutions of equation (1.2).

This is why homoclinic solution of (1.2) plays a crucial role in all mathematical studies of (1.1), and it is therefor useful to work out a (somewhat trivial) example of computing this homoclinic for $\Omega \in \mathbb{R}$, meaning u depends on time and one spatial variable only. We define a potential $W(u) = 2u^2(1+u)$, where $u = u(X,t)$ denotes the volume fraction of the polymer for each $X \in \Omega$.

We can scale the variable X by introducing $x = \varepsilon^{-1}X$ after which (1.2) becomes

$$u_{xx} - 4u + 6u^2 = 0. \quad (1.4)$$

This second-order differential equation has a solution $u_0(x,t) = \text{sech}^2(x)$, which is shown in Figure 2. This solution is an example of a *stationary pulse solution*: a solution that is time independent and consists of one or several peaks. The function $u_0(x,t)$ is the explicit form of a homoclinic solution to the origin in the (u, u_x) phase-plane, which is why we will usually denote it as the homoclinic solution of the system.

The interpretation of this solution is that anywhere but at the origin there is a very low concentration of polymers, whereas at the origin there is a peak in concentration. When extending to higher dimensions of Ω, this peak could represent a bilayer of polymers, meaning these stationary pulse solutions are of interest to us.

1.3 The two-component FCH

Most work on amphiphilic polymers revolve around the assumptions as above, where there is one polymer in a bulk solvent phase, represented by a volume

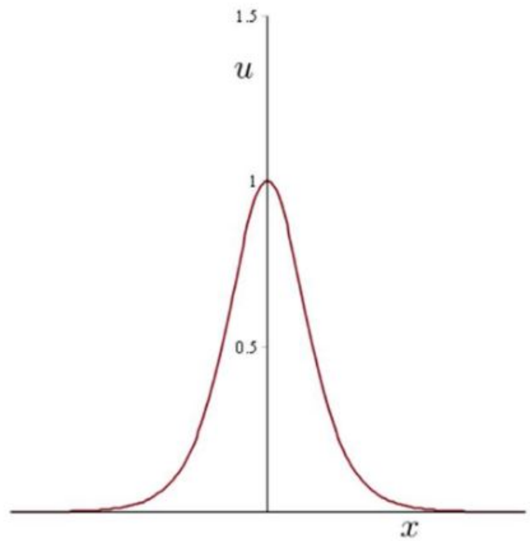

Figure 2: *The stationary pulse solution* $u = \text{sech}^2(x)$ *of equation* (1.4).

fraction u. In [2], the authors prove the existence of bilayers for any $d \geq 2$ and study the stability of these solutions, for instance.

For this thesis I will consider an extension of the model, where we look at two distinctly different amphiphilic polymers in a solvent. We describe the volume fractions of these polymers in the solvent with functions $u, v \in H^2(\Omega)$, and identical curvature assumptions as in the one-component case. We are once more interested in the existence of bilayers, but one can imagine the increased amount of possibilities that arise by introducing a second component. As the polymers are distinct, they have different shapes, sizes and behave chemically different.

We thus extend the model to a two-component case, which we call the multi-component functionalized Cahn-Hilliard free energy. The critical points of this free energy are now solutions of the two-dimensional extension of equation (1.3), hence with a vector $\vec{u} = (u, v)^T$. Since a 4-dimensional system of differential equations is needed to describe the dynamics of each polymer, solving this corresponds to solving an 8-dimensional differential equation. Since this is very difficult, we strive to reduce the problem somewhat in order to do some analysis on this multi-component case.

In the one-component case, we mentioned the importance of the homoclinic solution to equation (1.2). Solutions of this equation were close to minimizers of the one-component FCH, and it may be possible to extend this idea to the two-component case.

Thus we will try to find solutions to a two-dimensional extension of (1.2):

$$\varepsilon^2 D\Delta\vec{u} - \nabla W(\vec{u}) = \varepsilon T(\vec{u}), \tag{1.5}$$

where $\vec{u} = (u, v)^T$ now is a vector, D is a diffusion matrix and T is a vector field which we will specify later in this thesis. Because of the chemical differences between u and v mentioned above, the polymers diffuse at different speeds. We assume the following diffusion matrix

$$D = \begin{pmatrix} 1 & 0 \\ 0 & \delta \end{pmatrix},$$

which implies that v diffuses δ times slower than u.

Remark. This δ generally does not depend on the interface thickness ε, but we will later see that an assumption $\delta = \varepsilon^2$ is convenient for our analysis.

As u and v represent volume fractions, biologically relevant assumptions would be that $0 \leq u, v \leq 1$ and $u + v \leq 1$ everywhere. In this thesis I will **not** make these assumptions, because the point of interest of my research is not quantitative in nature but rather the existence of a specific type of solution. Furthermore, any eventual results can be scaled afterwards such that the restrictions are met.

To preserve the richness of the space of possible solutions the addition of a vector field $T(\vec{u})$ is necessary when the number of components is greater than one. To explain why, we need the following definition:

Definition. A vector field $V : \mathbb{R}^d \to \mathbb{R}^d$ is called *conservative* if there exists a function $v : \mathbb{R}^d \to \mathbb{R}$ for which

$$V = \nabla v$$

holds. For $d = 2$, any conservative function has curl zero, meaning

$$\frac{\partial V_2}{\partial x} - \frac{\partial V_1}{\partial y} = 0.$$

In one dimension, any integrable function V is conservative since the gradient is simply its primitive function, but this will not be the case in higher dimensions. Thus by only using a term $\nabla W(\vec{u})$ in (1.5), we restrict ourselves to only conservative functions, while there is no such restriction on the possible functions W' in (1.1) and (1.2).

By adding a **non-conservative** vector field $T(\vec{u})$, which is thus a field with curl zero, we preserve the richness of the solution space. However, we assume that this non-conservative vector field is $\mathcal{O}(\varepsilon)$ to remain close to the possibly more simple conservative situation.

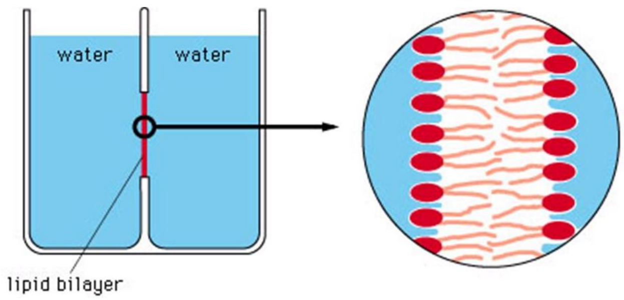

Figure 3: *A graphical display of a β-single curvature bilayer interface with $\beta = 0$, which corresponds to a flat bilayer.*

The (nonzero) function $W(u, v)$ is a function depending on u as well as v, and a logical extension from the one-component double-well $W(u)$ would be that this function should now have 3 local minima. The main focus of this thesis will however lie in finding a homoclinic to a specific background state, and will not focus to much on the global behavior of this function $W(u, v)$. Hence we will see that our choice for $W(u, v)$ is based more on its use for applying mathematical theory than on its biological correctness. In fact, the precise biological motivation underlying the multi-component FCH model is at present still strongly under construction. For example, in the recent article [8], the authors argue that it is not even necessary $W(u, v)$ is a potential. Nevertheless, I choose to study the direct generalization of (1.1) into 2 components with a potential $W(u, v)$.

We are interested in finding a stationary pulse solution of equation (1.5) for a general $d \geq 2$. To do this, we introduce a different coordinate system that fits the model better in the following paragraph.

1.3.1 Higher Dimensions: Curvilinear Coordinates

Because of the chemical relevance we are mainly interested in the existence of the lipid bilayers (see Figure 1) in this thesis, and hence we will try to form our mathematical model to these formations. To solve (1.2) for a general $d \geq 2$, it seems useful to make a change of coordinate system. Smooth interfaces of co-dimension one that are far from self-intersection admit a coordinate system that involves the distance to the interface, which we will denote with r. We assume the interface is of the simplest class, which are called β-single curvature interfaces, and correspond to higher order generalizations of cylinders and spheres where $\beta \in \{0, 1, \ldots, d-1\}$ denotes the number of curved directions. In three-dimensional space, spherical interfaces are an example of a single curvature interfaces with $\beta = 2$, whereas cylinders correspond to $\beta = 1$ and flat interfaces to $\beta = 0$. An example of a 2-single curvature interface is the spherical bilayer in Figure 1 (left), and an example of a flat bilayer is in Figure 3.

We now write the radius r as the sum of a constant R_0, denoting the radius of the β-single curvature interface, and a ε-scaled distance term R, hence we write $r = R_0 + \varepsilon R$. We do this because we are mainly interested in the behavior of the functions u and v in a neighborhood of the interface, which is $\mathcal{O}(\varepsilon)$ thick, so we focus on the R-term hereafter.

With the above assumptions, the Laplacian can be written such that it only depends on the first and second partial derivative with respect to R:

$$\varepsilon^2 \Delta = \partial_R^2 + \frac{\varepsilon\beta}{R_0 + \varepsilon R}\partial_R.$$

For more details on deriving this Laplacian, see [2].

Substituting this Laplacian into equation (1.5) and writing the system out for $\vec{u} = (u, v)^T$ and diffusion matrix D as defined above gives:

$$\begin{aligned} \frac{\partial^2 u}{\partial R} + \frac{\varepsilon\beta}{R_0 + \varepsilon R}\frac{\partial u}{\partial R} &= \frac{\partial W}{\partial u} + \varepsilon T_1(u, v) \\ \delta\left(\frac{\partial^2 v}{\partial R} + \frac{\varepsilon\beta}{R_0 + \varepsilon R}\frac{\partial v}{\partial R}\right) &= \frac{\partial W}{\partial v} + \varepsilon T_2(u, v), \end{aligned} \tag{1.6}$$

which will be the system we study in this thesis. The goal will be to find a stationary pulse solution (u_h, v_h) of (1.6) that is homoclinic to the origin, meaning $\lim_{R\to\pm\infty}(u_h, v_h) = (0, 0)$.

Solving system (1.6), a system of second-order differential equations, corresponds to solving 4 first-order differential equations, which is difficult to do with 'standard' phase plane analysis. We will apply geometric singular perturbation theory. This theory is mainly based on several fundamental results by Neil Fenichel, which we will introduce in chapter 2. We will see that with only a few small assumptions and adaptations to system (1.6), we can apply this geometric singular perturbation theory.

I will follow an approach used in *Pulses in a Gierer-Meinhardt Equation with a Slow Nonlinearity* by Veerman and Doelman ([9]), where a singularly perturbed 4-dimensional system similar to our thesis equations (1.6) is studied. However, the systems differ on several essential points, making the analysis different and leading to alternative results.

2 Geometric singular perturbation theory

2.1 Introduction

Geometric singular perturbation theory is a useful tool in analyzing systems that admit an evident separation of time scales, and uses invariant manifolds in phase space to understand the global phase space of the system. With the theory, it can be made possible to analyze singularly perturbed systems of double the size than can be analyzed without the theory. In other words, the theory makes it possible to analyze for example a 4-dimensional system of differential equations meeting some relatively general requirements, with techniques used for 2-dimensional systems. This makes geometric singular perturbation theory a very strong tool, as these 2-dimensional methods are better-known and generally less complicated.

The foundation of geometric singular perturbation theory are three theorems by Neil Fenichel, developed in the 1970s. When Fenichel published his theorems the results did not get any real recognition by the mathematical world, and made no significant impact. It was a couple of decades later, through the lecture notes *'Geometric Singular Perturbation Theory'* ([5]) by Christopher Jones that the significance of the results were recognized, as Jones took great care formulating and explaining the theory. Furthermore, the notes by Jones came with some new theorems and extensive examples, clarifying the scope of Fenichel's theorems.

There is another reason why Fenichel Theory is very useful for this thesis. As we mentioned earlier, we are looking for a stationary pulse solution, which corresponds to a homoclinic, or heteroclinic for that matter, orbit in phase space. One aspect of Fenichel Theory, and in particular the aspect explained in [4], focuses exactly on the construction of homoclinic or heteroclinic orbits of a dynamical system, by following manifolds of critical points through phase space. Thus this theory could lead us exactly where we want, given that we are able to construct these orbits from system (1.6).

The scope of this thesis does not involve the proofs of Fenichel's theorems, or extensive explanation about them. I will state the theorems and shortly explain why they are useful in general and specifically for this thesis. For a more elaborate explanation and a more extensive background on the theorems, I would like to refer to [4], [5] and [6].

2.2 Fenichel Theory

Suppose we have a system of the form

$$\begin{aligned} \varepsilon\frac{dx}{dt} &= f(x, y, \varepsilon) \\ \frac{dy}{dt} &= g(x, y, \varepsilon), \end{aligned} \tag{2.1}$$

where $\varepsilon \ll 1$, $x \in \mathbb{R}^k$ and $y \in \mathbb{R}^l$, with $k, l \geq 1$. We also assume that there exist $\tilde{x} \in \mathbb{R}^k$ and $\tilde{y} \in \mathbb{R}^l$ such that $f(\tilde{x}, \tilde{y}, 0) = 0$.

With a change of time scale $\tau = \frac{t}{\varepsilon}$ system (2.1) can be rewritten to

$$\begin{aligned} \dot{x} &= f(x, y, \varepsilon) \\ \dot{y} &= \varepsilon g(x, y, \varepsilon), \end{aligned} \tag{2.2}$$

where $\dot{}$ denotes taking the derivative with respect to the so-called *fast variable* τ. We can observe that these systems are identical for $\varepsilon \neq 0$, but when we set $\varepsilon = 0$ the systems (2.1) and (2.2) reduce to two different systems.

2.2.1 Fenichel's first theorem

Let $\varepsilon = 0$. Then system (2.2) reduces to a family of systems with k differential equations parametrized by $y = y_0 \in \mathbb{R}^l$ and we can find the fixed points of the reduced system. These are the points (x, y) for which $f(x, y, 0) = 0$, where we will be specifically interested in the hyperbolic fixed points. Hyperbolic fixed points are fixed points that do not have center manifolds, which means that the eigenvalues of the Jacobian matrix all have non-zero real parts. A family, or manifold, of hyperbolic fixed points is called a *Normally Hyperbolic Invariant Manifold* or NHIM, for short. Fenichel's first theorem states that a NHIM of the reduced system with certain properties, is close to a locally invariant manifold of the full system (2.1):

Theorem 2.1 (Fenichel's first theorem). *Suppose $M_0 \subseteq \{f(x, y, 0) = 0\}$ is compact, possibly with boundary, and normally hyperbolic, that is, the eigenvalues λ of the Jacobian $\frac{\partial f}{\partial x}(x, y, 0)|_{M_0}$ all satisfy $Re(\lambda) \neq 0$. Suppose f and g are smooth. Then for $\varepsilon > 0$ and sufficiently small, there exists a manifold M_ε, $\mathcal{O}(\varepsilon)$ close and diffeomorphic to M_0, that is locally invariant under the flow of the full problem* (2.1).

With this theorem we reduce the problem of finding a normally hyperbolic manifold of the full system, a system with $k + l$ differential equations, to finding a normally hyperbolic manifold of a system with k equations. In addition, by setting $\varepsilon = 0$ some terms may drop from the k differential equations, reducing the complexity of finding fixed points of the system.

Fenichel's first theorem not only gives us a result about the existence of the locally invariant manifold M_ε, but can also give us a way to construct this manifold from the invariant manifold M_0. The theorem states that M_ε is $\mathcal{O}(\varepsilon)$ close and diffeomorphic to M_0 so if M_0 is given by a graph of a function $p_0(y)$ then we can find a perturbation of this function that describes M_ε. In other words, if we found $M_0 = \{(x,y)|x = p_0(y)\}$ we can find a function p_ε such that $M_\varepsilon = \{(x,y)|x = p_0(y) + \varepsilon p_\varepsilon(y)\}$.

It is important to note that the manifold M_ε does not have to be unique and perhaps more importantly, that it generally does not consist of fixed points of the full problem. It is however locally invariant, which means orbits that start in M_ε can only leave the manifold in the slow direction.

2.2.2 Fenichel's second theorem

Suppose once more that $\varepsilon = 0$ and that M_0 is as in Fenichel's first theorem. Each $(x_0, y_0) \in M_0$ is a hyperbolic fixed point, meaning it has only eigenvalues with nonzero real part. Let the number of eigenvalues with negative real parts be n and the number of eigenvalues with positive real parts be p, such that $n + p = k$. Each equilibrium in M_0 then has a n-dimensional stable manifold $W^s((x_0, y_0))$ and p-dimensional unstable manifold $W^u((x_0, y_0))$, and these manifolds are invariant. We define

$$W^s(M_0) = \bigcup_{(x_0,y_0)\in M_0} W^s((x_0,y_0)) \quad \text{and} \quad W^u(M_0) = \bigcup_{(x_0,y_0)\in M_0} W^u((x_0,y_0))$$

as the stable and unstable manifold of M_0, respectively. Since M_0 is an l-dimensional manifold, we see that $W^s(M_0) \in \mathbb{R}^{l+n}$ and $W^u(M_0) \in \mathbb{R}^{l+p}$. Fenichel's second theorem now states that for $\varepsilon \ll 1$ there exist stable and unstable manifolds for the full system (2.1), with respect to the locally invariant set M_ε, that are a perturbation of $W^s(M_0)$ and $W^u(M_0)$:

Theorem 2.2 (Fenichel's second theorem)**.** *Suppose $M_0 \subseteq \{f(x,y,0) = 0\}$ is compact, possibly with boundary, and normally hyperbolic, that is, the eigenvalues λ of the Jacobian $\frac{\partial f}{\partial x}(x,y,0)|_{M_0}$ all satisfy $Re(\lambda) \neq 0$. Suppose f and g are smooth. Then for $\varepsilon > 0$ and sufficiently small, there exist manifolds $W^s(M_\varepsilon)$ and $W^u(M_\varepsilon)$, that are $\mathcal{O}(\varepsilon)$ close and diffeomorphic to $W^s(M_0)$ and $W^u(M_0)$, respectively, and that are locally invariant under the flow of* (2.1)*.*

As M_ε is not a collection of fixed points, the manifolds $W^s(M_\varepsilon)$ and $W^u(M_\varepsilon)$ are not stable and unstable manifolds in the sense that we are used to, but do behave similarly. Solutions in the 'stable' manifold $W^s(M_\varepsilon)$ have the property that they get close to M_ε at an exponential rate in forward time, whereas solutions in the 'unstable' $W^u(M_\varepsilon)$ get close to M_ε at an exponential rate in backward time.

2.2.3 Fenichel's third theorem

With Fenichel's first and second theorem, we have seen that for $\varepsilon \ll 1$, the manifolds M_0, $W^s(M_0)$ and $W^u(M_0)$ perturb to similar manifolds that are

$\mathcal{O}(\varepsilon)$ close. Recall that the stable and unstable manifolds of M_0 was defined as the collection of $W^{s,u}((x_0, y_0))$ respectively. We are now interested whether these individual manifolds also perturb to a similar object, especially since we will be looking for a specific orbit.

Let $(x_\varepsilon, y_\varepsilon) \in M_\varepsilon$ denote the perturbed counterparts of (x_0, y_0). We already stated that these points will in general not be fixed points for the full system (2.1), and thus the manifolds $W^{u,s}((x_\varepsilon, y_\varepsilon))$ will not be invariant either. Hence, whereas we have that $\lim_{t\to\infty} W^s((x_0, y_0)) = (x_0, y_0)$ exponentially, this will not be the case for its perturbed counterpart. The same holds for $W^u((x_\varepsilon, y_\varepsilon))$ in backward time. However, Fenichel's third theorem states that any point in $W^{u,s}(M_\varepsilon)$ has a point in M_ε associated to it, to which the manifolds decay exponentially in forward or backward time. But before we can state the theorem, we need the definition of the forward evolution of a set, as stated in [5]:

Definition. The forward evolution of a set $A \subset D$ restricted to D is given by the set

$$A \cdot_D t := \{x \cdot t : x \in A \text{ and } x \cdot [0, t] \subset D\},$$

where $x \cdot t$ denotes the application of a flow after time t to the initial condition x.

Theorem 2.3 (Fenichel's third theorem)**.** *Suppose $M_0 \subseteq \{f(x, y, 0) = 0\}$ is compact, possibly with boundary, and normally hyperbolic, and suppose f and g are smooth. Then for every $(x_\varepsilon, y_\varepsilon) \in M_\varepsilon$ with ε sufficiently small, there are a manifold $W^s((x_\varepsilon, y_\varepsilon)) \subset W^s(M_\varepsilon)$ and a manifold $W^u((x_\varepsilon, y_\varepsilon)) \subset W^u(M_\varepsilon)$, that are $\mathcal{O}(\varepsilon)$ close and diffeomorphic to $W^s((x_0, y_0))$ and $W^u((x_0, y_0))$ respectively. The families $\{W^{u,s}((x_\varepsilon, y_\varepsilon))|(x_\varepsilon, y_\varepsilon) \in M_\varepsilon\}$ are invariant in the sense that*

$$W^s((x_\varepsilon, y_\varepsilon)) \cdot_D t \subset W^s((x_\varepsilon, y_\varepsilon) \cdot t)$$

if $(x_\varepsilon, y_\varepsilon) \cdot s \in D$ for all $s \in [0, t]$, and

$$W^u((x_\varepsilon, y_\varepsilon)) \cdot_D t \subset W^u((x_\varepsilon, y_\varepsilon) \cdot t)$$

if $(x_\varepsilon, y_\varepsilon) \cdot s \in D$ for all $s \in [t, 0]$.

2.2.4 Application of Fenichel Theory

Above we have introduced the three theorems by Fenichel, but it is yet unclear how this theory will lead us to a homoclinic solution of the full system. To explain this and give a better notion on the application of Fenichel theorem, I will construct a stationary pulse solution of a three-dimensional singularly perturbed system in the following paragraph. The choice for a three-dimensional system is deliberate, because we will be able to show the final orbit graphically, which will not be the case with our four-dimensional thesis system.

Another deliberate choice is that the example has a heteroclinic orbit between two fixed points, whereas the goal of this thesis is the construction of a homoclinic orbit. This choice is once more made with visually attractive solutions in mind, and it must be noted that a homoclinic orbit is just a special version of a heteroclinic, meaning most of the analysis will be similar.

The system chosen is an adaptation of system (2.8) in [3], where the crucial difference is that the system in [3] has 2 distinctly different homoclinic orbits to the manifold M_ε, as opposed to just one in our example. This adaptation was made because we will see that thesis system (1.6) will also have just one homoclinic orbit to M_ε.

2.3 A 3-dimensional example

We consider the following 3-dimensional system of differential equations:

$$\begin{aligned} \varepsilon x' &= y \\ \varepsilon y' &= x - x^2 + \varepsilon y(z-1) \\ z' &= 1 + x - (cz)^2 \end{aligned} \quad , \tag{2.3}$$

where $0 \ll \varepsilon \ll c \ll 1$ and x, y, z are functions depending on the temporal variable t. We recognize that this system has the same form as (2.1), with $k = 2$ and $l = 1$, and thus we can apply Fenichel Theory. Introducing a variable $\tau = \frac{t}{\varepsilon}$ transforms (2.3) into

$$\begin{aligned} \dot{x} &= y \\ \dot{y} &= x - x^2 + \varepsilon y(z-1) \\ \dot{z} &= \varepsilon(1 + x - (cz)^2) \end{aligned} \quad , \tag{2.4}$$

which we call the *fast system*, as opposed to the *slow system* (2.3).

Following the lines of Fenichel Theory, we set $\varepsilon = 0$ and look at points (x, y, z) for which $f(x, y, z, 0) = 0$. In the case of system (2.4), we have

$$f(x, y, z, \varepsilon) = \begin{pmatrix} y \\ x - x^2 + \varepsilon y(z^2 - 1) \end{pmatrix},$$

and thus $f(x, y, z, 0) = (y, x - x^2)^T$, which is independent of z. The vector equals zero for $(x_1, y_1) = (0, 0)$ and $(x_2, y_2) = (1, 0)$ and thus the collections $M^1{:=}\{(x, y, z)|x = y = 0\}$ and $M^2{:=}\{(x, y, z)|x = 1, y = 0\}$ are sets of equilibrium points for (2.4) with $\varepsilon = 0$. From the determinant of the Jacobian matrix of the system we can conclude that the points in M^1 are saddle points, and the points in M^2 are center points. Note that both collections represent lines in the (x, y, z)-plane.

Since M^1 is a collection of saddle points, it is normally hyperbolic, and we can thus apply Fenichel Theory to it. The collection M^2 is on the other hand not normally hyperbolic, and we will not consider it any more in this example.

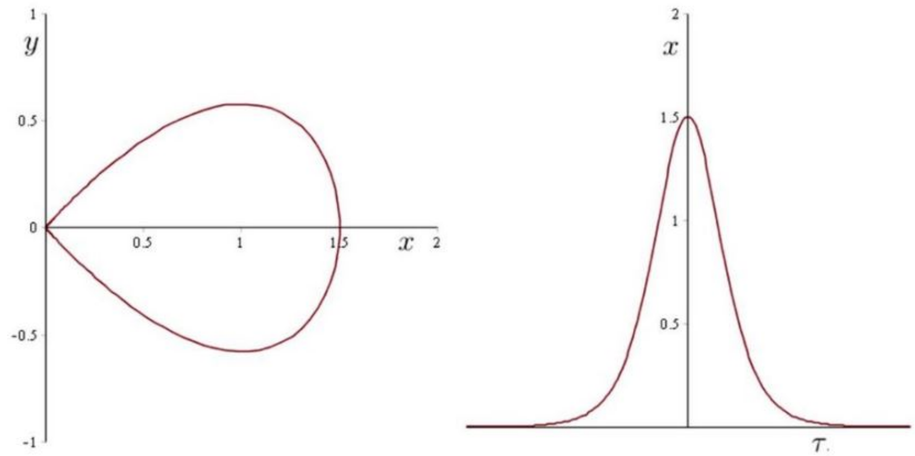

Figure 4: *The homoclinic solution to the point* $(x, y) = (0, 0)$ *of system* (2.4) *with* $\varepsilon = 0$ *in the phase-plane (left) and in the* (τ, x)*-plane (right).*

Continuing, we can determine the stable and unstable manifold of the saddle points in M^1, which we will denote with $W^s(M^1)$ and $W^u(M^1)$, respectively. We can recognize that system (2.4) with $\varepsilon = 0$ is a Hamiltonian system, which implies that the stable and unstable manifold of points in M^1 will coincide into a homoclinic orbit. The Hamiltonian function of the system is

$$H(x, y) := \frac{1}{2}y^2 - \frac{1}{2}x^2 + \frac{1}{3}x^3,$$

where we have that $H(0, 0) = 0$, meaning the homoclinic orbit must solve $H(x, y) = 0$ as well. Recalling that $y = \dot{x}$, this means the homoclinic orbit we are seeking must solve the following differential equation

$$\left(\frac{dx}{d\tau}\right)^2 = x^2 - \frac{2}{3}x^3.$$

The solution of this differential equation is $x_{h,0}(\tau) := \frac{3}{2}\operatorname{sech}^2(t/2)$, and together with $y_{h,0}(\tau) := \dot{x}_{h,0}(\tau)$ we have found a homoclinic solution to the equilibrium point $(x, y) = (0, 0)$. Figure 4 shows this homoclinic orbit, both in the (x, y) phase-plane as in the (τ, x)-plane.

Because M^1 did not just represent a single equilibrium point, but in fact a line of fixed points $(0, 0, z_0)$, the homoclinic we found is also a solution for any z_0. This means we actually have a family of homoclinic orbits $(x_{h,0}, y_{h,0}, z_0)$ for (2.4) with $\varepsilon = 0$ in the three-dimensional plane, see Figure 5 (left). Thus we have now found a collection of stationary pulse solutions for the system, but we are wondering what happens with this collection when $\varepsilon \neq 0$. This is where we are going to apply Fenichel Theory.

We have already concluded that M^1 is a collection of saddle points, meaning it is a normally invariant hyperbolic manifold. Thus, any compact subset M_0 of M^1 can be used for Fenichel's first theorem. Looking at system (2.4), we can see that setting $(x, y) = (0, 0)$ still leads to $\dot{x} = \dot{y} = 0$, so we can conclude that M_0 is also locally invariant under the flow of the full system. Note that M_0 is **not** a set of critical points for (2.4), as we do not have $\dot{z} = 0$ for general z. In fact, the only z for which $(x, y, z) \in M_0$ are equilibrium points of (2.4) are $z^*_\pm = \pm c^{-1}$.

From Fenichel's second theorem it now follows that the stable and unstable manifold of M_0 persist, but are $\mathcal{O}(\varepsilon)$ perturbed. Whereas for $\varepsilon = 0$ we had that the manifolds merged into a homoclinic orbit, they are now separated and coincide only on a finite number of places, possibly nowhere. Since we are interested in a homoclinic to M_0, it is exactly these intersections we are interested in. This homoclinic starts asymptotically close to M_0, follows the unstable manifold until it reaches an intersection, where it continues following the stable manifold back to M_0. I would like to remark that because $W^s(M_0)$ and $W^u(M_0)$ are two-dimensional manifolds, their intersections are one-dimensional manifolds.

These intersections can be found by determining the zeroes of the Melnikov function, a function used to denote the distance of the stable and unstable manifold in any plane $\{z = z_0\}$. In this chapter, I will omit a more extensive explanation of the Melnikov method and just pose the results. In chapter 4 I will explain the theory further, and do the calculations for the system we are studying in this thesis.

The Melnikov function has exactly one zero, located at $z = 1$, which means the stable and unstable manifold intersect and a homoclinic orbit to M_0 exists. Note that $z = 1$ is again not the exact location of the intersection for the full system, but just $\mathcal{O}(\varepsilon)$ close to it.

We now have a good notion of what happens in the fast field: a fast excursion away from M_0 at $z = 1$ in the form of a stationary pulse solution in the (τ, x)-plane. Now we are interested in the behavior of this orbit in the slow field, at the manifold M_0. Substituting $x = y = 0$ in (2.3) leaves the equation $z' = 1 - cz^2$. This equation has equilibrium points $z^\pm = \pm c^{-1}$, where z^- is an unstable node and z^+ is a stable node.

This now gives us an approximate idea of the stationary pulse solution of system (2.3): it is a heteroclinic orbit that goes to the unstable node $(x, y, z) = (0, 0, z^-)$ for $t \to -\infty$. It increases in the z-direction along the slow manifold M_0, until it reaches (a point $\mathcal{O}(\varepsilon)$ close to) $z = 1$, where the orbit takes a fast excursion through the fast (x, y)-plane. After returning to M_0 the orbit continues to increase slowly along the z-axis, where it finally goes to the stable node $(x, y, z) = (0, 0, z^+)$ for $t \to \infty$. Note that this orbit is a one-dimensional curve,

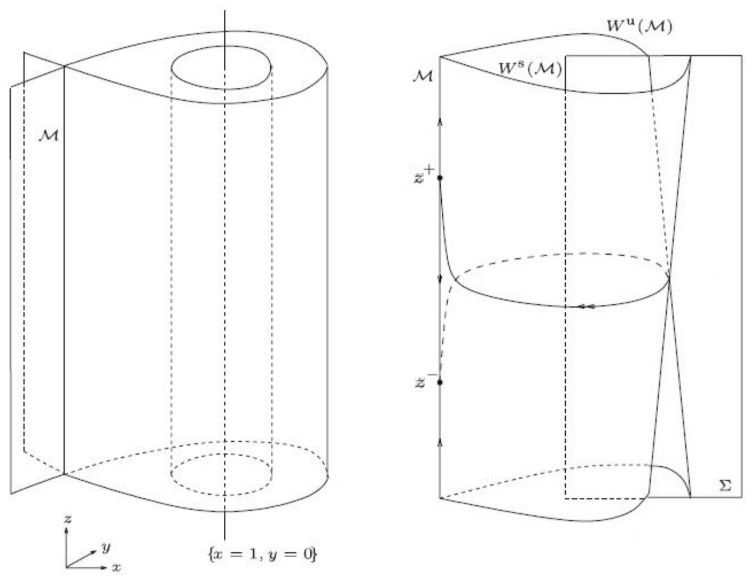

Figure 5: *The family of homoclinic orbits of system* (2.3) *to* $M = M_0$ *for* $\varepsilon = 0$ *(left) and the stable and unstable manifold to* $M = M_\varepsilon$ *with the heteroclinic orbit from* z^- *to* z^+ *for* $\varepsilon \neq 0$ *(right). The plane* Σ *is the cross-section* $\{y = 0\}$ *at which the* $W^{s,u}(M_\varepsilon)$ *intersect. Source: [4]*

since it is in the intersection of the two-dimensional stable and unstable manifolds of M_0. See Figure 5 (right).

Although this example was of lower dimension than the system we study in this thesis, the method for finding a homoclinic orbit of (1.6) will be done analogously. We will construct a fast homoclinic solution to a slow manifold M_0 of critical points, which will now be two-dimensional. Then we will study the behavior of orbits on this slow manifold and see if we can also find a slow homoclinic on this manifold. With Fenichel Theory, we will then 'glue' together the slow and fast parts together to a homoclinic of the full problem and use Fenichel Theory to ensure that this homoclinic exists under the $\mathcal{O}(\varepsilon)$ perturbation. This homoclinic will be an orbit that asymptotically connects the so-called background state $(u, v) = (0, 0)$ of the system to itself.

Remark. In the example we have said that when a system is Hamiltonian, the unstable and stable manifolds of a saddle equilibrium 'coincide' into a homoclinic orbit to this equilibrium. Although it is true that this homoclinic is a subset of both the stable and unstable manifold, it is not the entire manifold. There are parts of the stable and unstable manifold, in the case of the example for $x < 0$, that do not coincide. However, since we are only interested in the homoclinic solution, we will slightly abuse mathematical notation and state the manifolds coincide, for the remainder of this thesis.

2.4 Rewritting the thesis system to Fenichel's form

Recall system (1.6), the set of equations that we are studying in this thesis. We want to try and find a stationary pulse solution of these equations, by applying Fenichel Theory to the system. However, it is clear that system (1.6) is not yet in the correct form to apply the theory discussed in the previous paragraphs.

We start by writing the system as four first-order differential equations, instead of two second-order equations. To do this, we introduce the variables p and q such that $p := \frac{du}{dR}$ and $q := \sqrt{\delta}\frac{dv}{dR}$. Substituting this into (1.6) gives us

$$\begin{aligned} u' &= p \\ p' &= \frac{\partial W}{\partial u} + \varepsilon T_1(u,v) - \frac{\varepsilon\beta}{R_0 + \varepsilon R} \cdot p \\ \sqrt{\delta} v' &= q \\ \sqrt{\delta} q' &= \frac{\partial W}{\partial v} + \varepsilon T_2(u,v) - \frac{\varepsilon\beta}{R_0 + \varepsilon R} \cdot \sqrt{\delta} q, \end{aligned} \tag{2.5}$$

where $'$ denotes differentiation with respect to R. As mentioned in paragraph 1.3, the parameter δ generally does not depend on ε, but to be able to apply Fenichel Theory we make the assumption $\delta = \varepsilon^2$. This leads to a system that is of the same form as in Fenichel's theorems, with $k = l = 2$. Hence we can apply the theory to find a stationary pulse solution.

3 Exploring the system

3.1 Defining a potential

For this thesis, we define a potential function $W : \mathbb{R}^2 \to \mathbb{R}$, dependent on the volume fractions u, v and several parameters. The form of this potential is chosen mainly with the analysis method in mind, which means it does not directly meet the original biological motivations, as mentioned in chapter 1. However once more, this biological motivation and the form of the function W is presently still under construction, as also mentioned in [8].

We define the potential $W(u, v)$ as follows:

$$W(u,v) = \theta uv + \frac{1}{2}v^2 - \frac{2}{3\theta u}v^3 + \frac{1}{2}\alpha u^2 - \frac{\gamma}{n+1}u^{n+1}, \tag{3.1}$$

where $n > 2$. Furthermore, we take $\theta, \alpha > 0$ and $\gamma \in \mathbb{R}\backslash\{0\}$. The partial derivatives of this potential function are:

$$\begin{aligned} \frac{\partial W}{\partial u}(u,v) &= \theta v + \frac{2}{3\theta u^2}v^3 + \alpha u - \gamma u^n \\ \frac{\partial W}{\partial v}(u,v) &= \theta u + v - \frac{2}{\theta u}v^2. \end{aligned}$$

The goal of this thesis is finding a stationary pulse solution (u_h, v_h) that has $\lim_{t\to\pm\infty}(u_h, v_h) = (0, 0)$, which corresponds to finding an orbit homoclinic to the origin $(u, v) = (0, 0)$. We see that the potential $W(u, v)$ is not defined at the origin, due to the v^3/u-term, which means the origin is not an equilibrium point of the system. This would mean this point can not be in the critical manifold M_0 and Fenichel Theory can't actually be applied. In [1] the authors show for a similar system of equations that this will not be an issue, since $u = 0$ will be on the boundary of M_0 and we will only get asymptotically close to the origin. I will remark on this issue more at the end of paragraph 3.4, when we have done some initial analysis. We will see that the results from [1] can be extended to the system of this thesis, and thus we will sometimes with a slight abuse of notation say that the origin is an element of the manifold(s) M_ε.

Substituting the partial derivatives of $W(u, v)$ into (2.5) now gives us

$$\begin{aligned} u' &= p \\ p' &= \theta v + \frac{2}{3\theta u^2}v^3 + \alpha u - \gamma u^n + \varepsilon T_1(u,v) - \frac{\varepsilon\beta}{R_0 + \varepsilon R}\cdot p \\ \varepsilon v' &= q \\ \varepsilon q' &= \theta u + v - \frac{2}{\theta u}v^2 + \varepsilon T_2(u,v) - \frac{\varepsilon^2\beta}{R_0+\varepsilon R}\cdot q, \end{aligned} \tag{3.2}$$

which is the four-dimensional system we will be working with for the remainder of this thesis.

3.2 A specific choice of parameters

Before analyzing this system in full for general values of the parameters, it is useful to gain some knowledge about its behavior. Thus we will start with constructing a stationary pulse solution for a specific choice of parameters. First we make the assumption that the interface is of the simplest form, which is a flat bilayer, see again Figure 3. This means there is no curvature which corresponds with $\beta = 0$.

Furthermore, we choose $T_1 = T_2 = 0$. Since we purposely added this vector field to our equation to enrich the solution space, this assumption is now only made to simplify the system and analyze it. Later we will continue the analysis with a more general vector field T. With these assumptions, the system more resembles the slowly linearized Gierer-Meinhardt equation discussed in [9], making it more simple to follow the approach from the article. Furthermore, it will give us a chance to familiarize ourselves with the roles of the remaining parameters and the methods of Fenichel Theory for a four-dimensional system. Note that the terms that drop by this choice of parameters are all of $\mathcal{O}(\varepsilon)$ or higher, which means the analysis for $\varepsilon = 0$ remains analogously even for general values of the parameters.

Consider system (3.2), with $\beta = T_1 = T_2 = 0$:

$$\begin{aligned} u' &= p \\ p' &= \theta v + \frac{2}{3\theta u^2} v^3 + \alpha u - \gamma u^n \\ \varepsilon v' &= q \\ \varepsilon q' &= \theta u + v - \frac{2}{\theta u} v^2, \end{aligned} \tag{3.3}$$

where $'$ denotes taking the derivative with respect to R. We recognize that this is a system of the form required for applying Fenichel Theory, the form of (2.1), with $y = (u, p)^T$, $x = (v, q)^T$ and thus $k = l = 2$.

We start our analysis by making a so-called slow-fast decomposition, which means we will look at two different spatial scales, resulting in a 'slow' and a 'fast' system. Note that although the system we are working with involves a spatial variable, we will still use the terminology associated with temporal variables, and thus use terms such as slow and fast.

To do this slow-fast decomposition, we introduce a new spatial variable $\xi = \frac{R}{\varepsilon}$ and substitute this into system (3.3). This gives us

$$\begin{aligned} \dot{u} &= \varepsilon p \\ \dot{p} &= \varepsilon \left(\theta v + \frac{2}{3\theta u^2} v^3 + \alpha u - \gamma u^n \right) \\ \dot{v} &= q \\ \dot{q} &= \theta u + v - \frac{2}{\theta u} v^2, \end{aligned} \tag{3.4}$$

where $\dot{}$ denotes differentiation with respect to the new variable ξ. We denote R as the 'slow' variable and ξ as the 'fast' variable, and from now on we will refer to (3.3) as the **slow system** and to (3.4) as the **fast system**.

Note that the slow and fast system are equivalent for $\varepsilon \neq 0$, because they are just transformations of one another, but differ for $\varepsilon = 0$. Setting ε to zero, reduces both systems to a different two-dimensional dynamical system, where both can give us some interesting information about the behavior of the full system.

Thus we start by setting $\varepsilon = 0$ and doing this results in the *reduced slow system*

$$\begin{aligned} u' &= p \\ p' &= \theta v + \frac{2}{3\theta u^2}v^3 + \alpha u - \gamma u^n \\ 0 &= \theta u + v - \frac{2}{\theta u^2}v^2 = q, \end{aligned} \tag{3.5}$$

and the corresponding *reduced fast system*:

$$\begin{aligned} \dot{u} &= \dot{p} = 0 \\ \dot{v} &= q \\ \dot{q} &= \theta u + v - \frac{2}{\theta u}v^2. \end{aligned} \tag{3.6}$$

In correspondence with Fenichel Theory, we will start our analysis by looking at fixed points (u^*, p^*, v^*, q^*) of the reduced fast system. We will then see if the system has a normally hyperbolic invariant manifold M_0 and construct a homoclinic solution $(u_{h,0}, v_{h,0})$ to this manifold. Later we will use Fenichel theory to draw conclusions about this homoclinic solution for the full system (3.3).

3.3 Analyzing the reduced fast system

To analyze the reduced fast system we will search for equilibria of the system and then find out their nature. Finding the nature of the equilibria e.g. finding out if a fixed points is attracting, repelling, hyperbolic etc. is essential because Fenichel's theorems can only be applied to hyperbolic fixed points. The system is in equilibrium when all derivatives equal zero, which holds for general initial conditions $(u(0), p(0)) = (u_0, p_0)$.

The v-direction equals zero if and only if $q = 0$. Lastly, for the q-direction, we must solve

$$\theta u_0 + v - \frac{2}{\theta u_0}v^2 = 0,$$

where we used that the u-coordinate does not change in the fast field, so $u(\xi) = u_0$. With the quadratic formula we find that $v = \theta u_0$ and $v = -\frac{1}{2}\theta u_0$ are the zeroes of $\dot{q} = 0$.

So we find that there are two sets of equilibria of the reduced fast system: $\tilde{M}$:=$\{(u,p,v,q)|u\neq 0, v=\theta u, q=0\}$ and $\hat{M}$:=$\big\{(u,p,v,q)\big|u\neq 0, v=-\frac{1}{2}\theta u, q=0\big\}$. Note that these sets represent planes in the (u,p,v,q)-plane, since the equilibria hold for general initial conditions u_0, p_0. We can find the local nature of these fixed points by linearizing the system around these points, hence we compute the Jacobian matrix of the system. The Jacobian matrix at a fixed point (v^*, q^*) equals

$$J(v^*,q^*) = \begin{pmatrix} 0 & 1 \\ 1-\frac{4}{\theta u_0}v^* & 0 \end{pmatrix},$$

so for any fixed point we get that $\det(J(v^*,q^*)-\lambda \mathrm{I})=0$ for

$$\lambda_{\pm} = \pm\sqrt{1-\frac{4}{\theta u_0}v^*}.$$

So for $v^*=\theta u_0$ we get $\lambda_\pm = \pm\sqrt{3}i$ meaning the set $\tilde{M}$ is filled with centers or spirals. For $v^* = -\frac{1}{2}\theta u_0$ we get $\lambda_\pm = \pm\sqrt{3}$ meaning $\hat{M}$ is filled with saddle points. Thus $\hat{M}$ is a hyperbolic normally invariant manifold of the reduced fast system, which means that any compact subset $M_0 \subset \hat{M}$ can be used for applying Fenichel Theory. Of course, since we are interested in the behavior of the system in a neighborhood of $(u,p,v,q)=(0,0,0,0)$, a sufficiently large area around the origin should be in M_0. For instance we could take

$$M_0 = \left\{(u,p,v,q)\middle| 0<u<\varepsilon^{-2}, v=-\frac{1}{2}\theta u, q=0\right\},$$

especially since values $u<0$ have no biological relevance.

Now that we have found a set of hyperbolic fixed points of (3.4), we are interested in finding the stable and unstable manifolds of these points. We see that $\dot{v}$ is only dependent of the variable q and $\dot{q}$ is only dependent of the variable v (and the constant $u=u_0$), so we recognize the system as a Hamiltonian system. This means it has an energy function $H(v,q)$ along which the orbits have a constant value H. This *Hamiltonian function* equals

$$H(v,q) := \frac{1}{2}q^2 - \theta u_0 v - \frac{1}{2}v^2 + \frac{2}{3\theta u_0}v^3.$$

We are interested in homoclinic orbits to the hyperbolic fixed points in M_0, hence we substitute the equilibrium $(v^*,q^*) = \left(-\frac{1}{2}\theta u_0, 0\right)$ into the Hamiltonian function. This leads to finding that $H(v^*,q^*) = \frac{7}{24}(\theta u_0)^2$. Thus the entire orbit of (v^*,q^*) has this same energy, which means the homoclinic orbit $(v_{h,0}, q_{h,0})$ to (v^*,q^*) must solve

$$q^2 = 2\theta u v + v^2 - \frac{4}{3\theta u_0}v^3 + \frac{7}{12}(\theta u_0)^2,$$

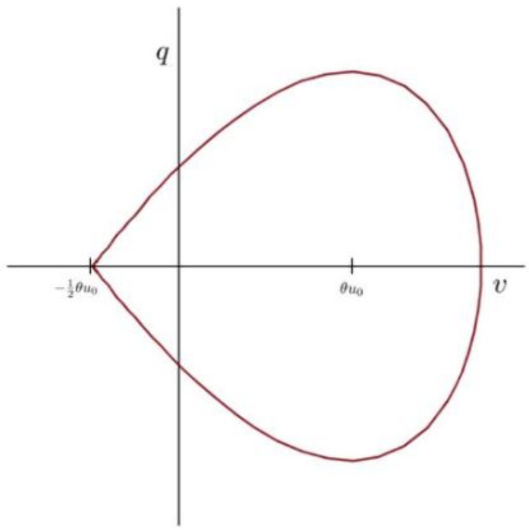

Figure 6: *A plot of the homoclinic orbit* $(v_{h,0}, q_{h,0})$ *for a general value of* θu_0.

where the subscript $v_{h,0}$ and $q_{h,0}$ indicates that this is the homoclinic of the reduced system, hence the system with $\varepsilon = 0$. Note that this homoclinic depends on ξ as well as the initial conditions (u_0, p_0), meaning it is actually of the form $(v_{h,0}(\xi, u_0, p_0), q_{h,0}(\xi, u_0, p_0))$, but we will usually use shorter notations.

Because we defined $q = \dot{v}$ we actually have the equation

$$\left(\frac{dv}{d\xi}\right)^2 = 2\theta u_0 v + v^2 - \frac{4}{3\theta u_0} v^3 + \frac{7}{12}(\theta u_0)^2, \tag{3.7}$$

of which a parametric plot is given in Figure 6. We can find the homoclinic solution explicitly by solving this differential equation but doing this analytically proves to be difficult. Instead, we will try to deduce the form of the solution intuitively and then check this ansatz against the differential equation. We will do this by making good use of the phase plane picture in the (v, q)-plane. Here we found that the homoclinic has limits $-\frac{1}{2}\theta u_0$ for $\xi \to \pm\infty$ and reaches its maximal v-value v_{max} at $\xi = 0$. The latter holds because of the symmetry of the reduced fast system, so the transformation $\xi \mapsto -\xi$ leaves the system the same (only with reversed directions of the flow). We observe that the v-coordinate is maximal at $q = 0$, meaning $2\theta u_0 v_{max} + v_{max}^2 - \frac{4}{3\theta u_0} v_{max}^3 + \frac{7}{12}(\theta u_0)^2 = 0$.

Using that $v = -\frac{1}{2}\theta u_0$ is a double zero we can simplify the equation to

$$\left(v_{max} + \frac{1}{2}\theta u_0\right)^2 \left(v_{max} - \frac{7}{4}\theta u_0\right) = 0.$$

This gives us $v_{max} = \frac{7}{4}\theta u_0$.

Thus we are looking for a symmetrical function $v_{h,0}(\xi)$ with an existing limit and a maximum at $\xi = 0$. From our experience with stationary pulse solutions we know that such a function exists and that it has the form

$$v_h(\xi) = a\,\mathrm{sech}^b(c\xi) + d.$$

This function has $\lim_{\xi\to\pm\infty} v_h(\xi) = d$ and has a maximum $v_{max} = a + d$. So with our system we have that $d = -\frac{1}{2}\theta u_0$ and because $v_{max} = \frac{7}{4}\theta u_0$ we get $a = v_{max} - d = \frac{9}{4}\theta u_0$. We determine the value of b by using that for $y = \mathrm{sech}^b(x)$ we have

$$\left(\frac{dy}{dx}\right)^2 = b^2\left(y^2 - y^{2+\frac{2}{b}}\right)$$

We then use that the highest power of v in (3.7) is 3, meaning we need to have $2 + \frac{2}{b} = 3$, hence when $b = 2$. This means we now have the expression $v_{h,0}(\xi) = \theta u_0\left(\frac{9}{4}\mathrm{sech}^2(c\xi) - \frac{1}{2}\right)$ and by substitution we find that $c = \frac{\sqrt{3}}{2}$. Calculations of both the derivative of $y = \mathrm{sech}^b(x)$ and c can be found in Appendix A.

Thus we have now found a homoclinic solution $(v_{h,0}, q_{h,0})$ to the equilibrium point (v^*, q^*) for intitial conditions (u_0, p_0), where

$$v_{h,0}(\xi) = \theta u_0\left(\frac{9}{4}\mathrm{sech}^2\left(\frac{\sqrt{3}}{2}\xi\right) - \frac{1}{2}\right), \tag{3.8}$$

and $q_{h,0}(\xi) = \dot{v}_{h,0}(\xi)$. A plot of this pulse in the (ξ, v)-plane is shown in Figure 7.

This homoclinic orbit holds for any point in M_0, and we thus have a family of homoclinic orbits. When an equilibrium has a homoclinic orbit, its stable and unstable manifolds coincide and are described by exactly this homoclinic. Thus $W^s((v^*, q^*)) = W^u((v^*, q^*)) = (v_{h,0}, q_{h,0})$ for each equilibrium in M_0, meaning we can define:

$$W^s(M_0) = W^u(M_0) := \bigcup_{(u,p,v,q)\in M_0} (v_{h,0}, q_{h,0})$$

as the stable and unstable manifold of the critical manifold M_0. Although these manifolds are similar to the ones we defined in the 3-dimensional example in paragraph 2.3, it is important to note that $W^{s,u}(M_0)$ in this chapter are three-dimensional manifolds. This means their intersection will be of dimension 2.

We have now found a compact critical manifold filled with equilibrium points, and a family of homoclinic orbits to this manifold, for the reduced fast system. Now we can apply Fenichel Theory to draw conclusions on the persistence of these objects when we let $\varepsilon \neq 0$.

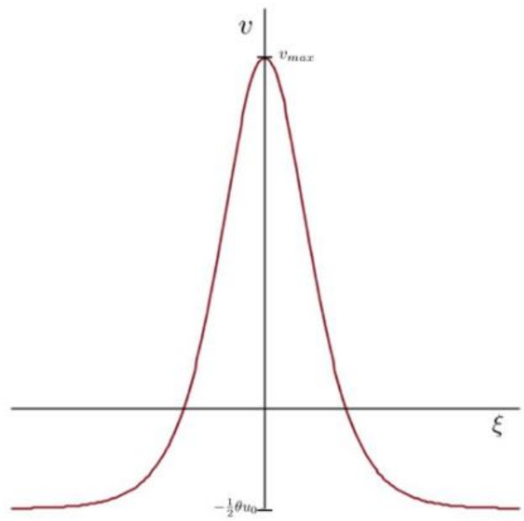

Figure 7: *A plot of the homoclinic $v_h(\xi)$ for a general θu_0. This figure is equivalent to the function in figure 6.*

Fenichel's first theorem ensures us that there exists a manifold M_ε $\mathcal{O}(\varepsilon)$ close and diffeomorphic to M_0 that is locally invariant under the flow of the full problem. Since the v- and q-equations of system (3.4) do not depend on ε, the manifold M_0 is still locally invariant under the flow of the full problem, meaning we can take $M_\varepsilon = M_0$. Note once more that this manifold is not a critical manifold, because the u- and p-equations will generally not be equal to zero.

From Fenichel's second theorem it now follows that there exist stable and unstable manifolds $W^{s,u}(M_\varepsilon)$ that are $\mathcal{O}(\varepsilon)$ close and diffeomorphic to $W^{s,u}(M_0)$, respectively, and that are locally invariant under the flow of the full system (3.4). We saw that for $\varepsilon = 0$ the manifolds $W^{s,u}(M_0)$ coincide into three-dimensional union of a family of homoclinics. When we now let $\varepsilon > 0$ the stable and unstable manifolds will not coincide anymore, but are separated and intersect only on a finite number of places, if anywhere at all. Because the stable and unstable manifolds of M_ε are 3-dimensional, their intersections will be planes.

We know that the manifolds $W^{s,u}(M_\varepsilon)$ still intersect the v-axis in the (v,q)-plane so we will look for this intersection at the hyperplane $\{q = 0\}$, and thus we are looking to find $W^s(M_\varepsilon) \cap W^u(M_\varepsilon) \cap \{q = 0\}$. We will find this intersection along the lines of adiabatic Melnikov Theory, a theory that lets one compute the distance between the stable and unstable manifold measured at a certain cross section Σ. If this distance equals zero somewhere on this cross section Σ, we know the stable and unstable manifold intersect.

The most powerful feature of the Melnikov method is that it computes the distance between the stable and unstable manifold of a point of the full system but only uses the Hamiltonian function and homoclinic solution of the unperturbed problem. What the Melnikov method basically does is compute the change accumulated by the Hamiltonian $H(u,p,v,q)$ evaluated at $(u_0, p_0, v_{h,0}, q_{h,0})$ over the entire range of ξ, which we will denote by ΔH and is equal to:

$$\Delta H = \int_{-\infty}^{\infty} \frac{dH}{d\xi}(u_0, v_{h,0}, q_{h,0})\,\mathrm{d}\xi.$$

The derivative of $H(u,p,v,q)$ with respect to ξ, which we will denote as $\dot{H}$ is

$$\begin{aligned}\dot{H} = &\quad q\dot{q} - \theta\left(\dot{u}v + u\dot{v}\right) - v\dot{v} + \frac{2}{3\theta}\left(\frac{3v^2}{u}\dot{v} - \frac{v^3}{u^2}\dot{u}\right)\\ = &\quad q\dot{q} - \dot{v}\left(\theta u + v - \frac{2}{\theta u}v^2\right) - \dot{u}\left(\theta v + \frac{2}{3\theta u^2}v^3\right)\\ = &\quad -\varepsilon p\left(\theta v + \frac{2}{3\theta u^2}v^3\right),\end{aligned}$$

where we used the equations for $\dot{u}$, $\dot{v}$ and $\dot{q}$ from (3.4). We now evaluate this expression on the homoclinic $(u_0, p_0, v_{h,0}, q_{h,0})$ by substituting the explicit formulas we found into the above expression, and integrate this over ξ. We thus find that

$$\Delta H = -\varepsilon p_0 \int_{-\infty}^{\infty} \theta v_{h,0} + \frac{2}{3\theta u_0^2} v_{h,0}^3\,\mathrm{d}\xi,$$

is the distance between the stable and unstable manifolds of M_ε on the hyperplane $\{q = 0\}$.

Adiabatic Melnikov Theory now states that the simple zeroes of this so-called Melnikov Integral correspond to transverse intersections of the stable and unstable manifolds $W^{s,u}(M_\varepsilon)$. ΔH has a simple zero at $p_0 = 0$, which means a transversal intersection between $W^s(M_\varepsilon)$ and $W^u(M_\varepsilon)$ exists at $\{q = 0\}$. Thus we can conclude that homoclinic solutions to M_ε still exists.

However, unlike the 3-dimensional example in paragraph 2.3, the intersection of $W^s(M_\varepsilon)$ and $W^u(M_\varepsilon)$ is two-dimensional, meaning it contains a family of orbits homoclinic to M_ε. However, there is no guarantee that one of these orbits is homoclinic to the point $(0,0,0,0) \in M_\varepsilon$. Hence, what remains is figuring out whether such a particular orbit to the homoclinic orbit exists in the intersection of $W^{s,u}(M_\varepsilon)$. We thus need to better understand the dynamics of the system on the slow manifold M_ε and research the behavior of orbits on this manifold.

3.4 The slow system on M_ε

We now look at the dynamics of the full system on the manifold M_ε and determine this flow by substituting $q = 0$ and $v = -\frac{1}{2}\theta u$ in (3.3), which results in

$$\begin{aligned} u' &= p \\ p' &= \left(\alpha - \frac{7}{12}\theta^2\right) u - \gamma u^n. \\ q' &= v' = 0 \end{aligned} \tag{3.9}$$

Note that we have stopped using the notation u_0 here, because the u-coordinate is not constant anymore on the slow manifold.

The latter two equations of (3.9) are trivial, with solutions $v = v_0, q = q_0$, so we will focus mainly on the first two equations and evaluate these as a two-dimensional system. This system has equilibria $(u,p) = (0,0)$ and $(u,p) = (\overline{u}, 0)$, where $\overline{u} = (\nu/\gamma)^{\frac{1}{n-1}}$. Here we have introduced $\nu := \alpha - \frac{7}{12}\theta^2$, and to avoid that $\overline{u}$ has only imaginary values for odd n we assume that $\nu/\gamma > 0$. This holds for two parameter regions:

1. $\gamma > 0$ and $\alpha > \frac{7}{12}\theta^2$,
2. $\gamma < 0$ and $0 < \alpha < \frac{7}{12}\theta^2$.

We will assume the parameters to fall into the first region, meaning $\gamma, \nu > 0$. Later in this chapter we will see that parameter region 2 gives undesirable results and is thus useless for this thesis.

We see that the system has a different amount of equilibria depending on whether n is odd or even: for n odd $(\overline{u})^{n-1}$ has two distinct real solutions, for n even it has only one real solution. Since we are interested only in values of $u \geq 0$, we will neglect the negative solution.

We are once more interested in the nature of the equilibria of the system and do this again by linearizing the system around a general fixed point (u^*, p^*). The Jacobian matrix now equals

$$J(u^*, p^*) = \begin{pmatrix} 0 & 1 \\ \nu - n\gamma(u^*)^{n-1} & 0 \end{pmatrix},$$

and find that $\det(J(u^*, p^*) - \lambda \mathrm{I}) = 0$ for

$$\lambda_\pm = \pm\sqrt{\nu - n\gamma\,(u^*)^{n-1}}.$$

We assumed that $\nu > 0$ so we get that the Jacobian matrix at $(u^*, p^*) = (0,0)$ has real eigenvalues of opposite sign, meaning the origin is a saddle point on the slow manifold M_ε. Furthermore, if we evaluate the Jacobian matrix at the equilibrium $(u^*, p^*) = (\overline{u}, 0)$, we see it has eigenvalues $\lambda_\pm = \pm\sqrt{\nu(1-n)}$, which are purely imaginary because $n > 1$. This means that the latter equilibrium is a center or spiral, meaning the critical points on the slow manifold are of the same nature as the ones we found in the fast field.

Now, because u' and p' only depend on p and u respectively, we can recognize that this system is once more a Hamiltonian system, with energy function

$$H_2(u,p) = \frac{1}{2}p^2 - \frac{\nu}{2}u^2 + \frac{\gamma}{n+1}u^{n+1}.$$

Thus the Hamiltonian function passing through the fixed point $(u,p) = (0,0)$ represents a homoclinic solution to this point which we can write implicitly as

$$p = \pm u\sqrt{\nu - \frac{2\gamma}{n+1}u^{n-1}} \tag{3.10}$$

In *Pulses in singularly perturbed reaction-diffusion systems* by Frits Veerman ([9]) an equation with a Hamiltonian function where only the constants differ is solved explicitly. Thus we can use the results from this text and get that

$$u_{h,0}(R) = \left[\frac{\nu(n+1)}{2\gamma}\,\text{sech}^2\left(\frac{1}{2}(n-1)\sqrt{\nu}R\right)\right]^{\frac{1}{n-1}},$$

and $p_{h,0}(R) = u'_{h,0}(R)$ is a homoclinic solution on M_ε to the origin. To see the proof that this $u_{h,0}(R)$ indeed solves equation (3.10) I refer to Appendix A.

With help of the above we can see why parameter values from region 2 are not useful to us: when $\gamma < 0$, the eigenvalues of the linearized system in the origin are purely imaginary, meaning the origin is a center (or spiral). In this case the point $(\overline{u}, 0)$ is the saddle point, which implies the system has a homoclinic orbit to this point. Since the goal of this thesis was finding a stationary solution to the origin, parameters values from region 2 are of no use to us. Biologically this option is senseless as well: it suggest high concentration of polymer v everywhere but at the interface.

Before we go any further in finding a stationary pulse solution to the full system (3.3), let us reflect for a moment about what we now know, and see what more needs to be done. First we found a normally hyperbolic invariant manifold M_0 and constructed a homoclinic $(v_{h,0}, q_{h,0})$ to this manifold, where we had $\varepsilon = 0$. The union of these homoclinics over points in M_0 then formed the three-dimensional hyperplane $W^s(M_0) \cap W^u(M_0)$. By applying Fenichel Theory we then constructed a slow manifold M_ε that is locally invariant under the flow of the full system, so for $\varepsilon \neq 0$. We then used Melnikov Theory to prove the existence of a transversal intersection $W^s(M_\varepsilon) \cap W^u(M_\varepsilon) \cap \{q = 0\}$ at $p_0 = 0$, which also proves the existence of homoclinic orbits to the manifold M_ε. When we then looked closer at the slow dynamics at M_ε, we found that on this manifold, a homoclinic to the origin exists.

What now remains is finding precisely that orbit from $W^s(M_\varepsilon) \cap W^u(M_\varepsilon)$ that is homoclinic to M_ε, and also homoclinic to the origin $(u, p, v, q) = (0, 0, 0, 0)$. Thus we want to find an orbit that starts asymptotically close to the origin on M_ε and then follow the slow homoclinic $(u_{h,0}, p_{h,0})$. Then, close to $p = 0$, the orbit will take off from the slow manifold and make a fast excursion following $(v_{h,0}, q_{h,0})$. Lastly the orbit touches down on the slow manifold once more and continue following the slow homoclinic. Hence we are interested in where at M_ε the fast homoclinic takes off and where it touches down again.

These so-called *take-off* and *touchdown* sets follow from Fenichel's third theorem, and for more information on their construction and mathematical background, I would like to refer the reader to [5] and [6].

We define the take-off set $T_o \subset M_\varepsilon$ to be the collection of base points of all orbits in $W^u(M_\varepsilon)$ that have points in the intersection $W^s(M_\varepsilon) \cap W^u(M_\varepsilon)$. In the same manner we define the touchdown set $T_d \subset M_\varepsilon$ to be the collection of base points of all orbits in $W^s(M_\varepsilon)$ that have points in the intersection $W^s(M_\varepsilon) \cap W^u(M_\varepsilon)$. In other words, the points in T_o and T_d are all starting and ending points (asymptotically) in M_ε of the bi-asymptotic orbits in $W^u(M_\varepsilon) \cap W^s(M_\varepsilon)$.

On the manifold M_ε we have $p_\xi = \mathcal{O}(\varepsilon)$ meaning the p-coordinate on M_ε remains constant to leading order on the excursion through the fast field, which is spanned by the v- and q-directions. We are therefor only interested in the change the p-coordinate accumulates away from M_ε, during the excursion of the orbit through the fast field. We will denote this change with $\Delta_\xi p$, and we can calculate this change by integrating the equation for p_ξ over a specifically chosen interval.

We choose the following interval

$$I_f := \left\{ \xi \in \mathbb{R} \middle| |\xi| < \frac{1}{\sqrt{\varepsilon}} \right\}.$$

This choice of interval is such that it is asymptotically large with respect to the fast variable ξ, meaning the interval is large enough to incorporate all the change accumulated on the fast dynamics, and asymptotically small with respect to the slow variable R, which means we don't incorporate any change accumulated on the slow dynamics, to leading order.

Thus, the change in p (in forward time) of the pulse is given by

$$\begin{aligned}\Delta_\xi p &= \int_{I_f} p_\xi \, \mathrm{d}\xi = \varepsilon \int_{I_f} \theta v + \frac{2}{3\theta u^2} v^3 + \alpha u - \gamma u^n \, \mathrm{d}\xi \\ &= 2u_0 \sqrt{\varepsilon} \left(\nu - \gamma u_0^{n-1} \right) + \mathcal{O}(\varepsilon),\end{aligned}$$

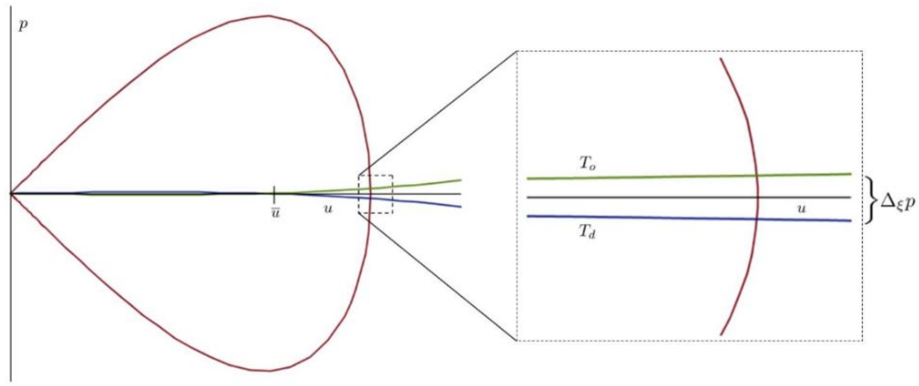

Figure 8: *Plots of the homoclinic solution* $(u_{h,0}, p_{h,0})$ *and the take-ff and touchdown curves for parameter values* $n = 3$, $\nu = 2$, $\gamma = 1$ *and* $\varepsilon = 10^{-4}$. *On the left is the full homoclinic and curves, whereas on the right we have zoomed in on the intersections of the homoclinic with the take-off and touchdown curves. This is where the jump through the fast field will take place.*

where a detailed calculation of this value can be found in Appendix A. Note that $\dot{u} = \varepsilon p$ and $p = \mathcal{O}(\sqrt{\varepsilon})$ on I_f, which implies that $\Delta_\xi u = \mathcal{O}(\varepsilon\sqrt{\varepsilon})$. This means the u-coordinate does not change to leading order during the excursion through the fast field compared to the change in p, meaning this excursion will go straight up or down in the (u, p)-plane.

We observe that $\Delta_\xi p$ equals zero in $u = 0$ and $u = \overline{u}$, where we denoted $\overline{u}$ as the u-coordinate of the center equilibrium point of the reduced slow system. Between these points $\Delta_\xi p$ is positive and for $u > \overline{u}$ it is negative. Note that a negative value of $\Delta_\xi p$ corresponds to a jump downward in the (u, p)-plane.

We found that the transversal intersection $W^s(M_\varepsilon) \cap W^u(M_\varepsilon) \cap \{q = 0\}$ is situated at (or $\mathcal{O}(\varepsilon)$ close to) $p = 0$ and thus the jump through the fast field occurs symmetrically around this hyperplane. This means the take-off and touchdowns sets can be described as the following curves, to leading order:

$$T_d := \left\{(u, p, 0, 0) | p = \ \ u\sqrt{\varepsilon}\left(\nu - \gamma u^{n-1}\right)\right\}$$
$$T_o := \left\{(u, p, 0, 0) | p = -u\sqrt{\varepsilon}\left(\nu - \gamma u^{n-1}\right)\right\}.$$

We can see that these sets are $\Delta_\xi p$ away from each other at each u, and that the jump is downward for $u > \overline{u}$.

Since the curves are of $\mathcal{O}(\sqrt{\varepsilon})$ and the homoclinic orbit $(u_{h,0}, p_{h,0})$ is of $\mathcal{O}(1)$, there exists a value $u^* > 0$ where the take-off and touchdown curves intersect this homoclinic. Since we are mainly interested in the existence of this intersection and not its exact location, we will not compute it explicitly. The take-off and touchdown curves are plotted togehter with the homoclinic solution $(u_{h,0}, p_{h,0})$ in Figure 8.

Let R^* be the **positive** R-value for which $u_{h,0}(R) = u^*$. We can now state the main existence theorem for system (3.4):

Theorem 3.1 (Existence of a stationary pulse solution)**.** *Let $\varepsilon > 0$ be sufficiently small. Then, for all values of the parameters $\theta > 0,\ \gamma > 0,\ \alpha > \frac{7}{12}\theta^2$ and $n > 1$, there exists a unique orbit $\chi_h(\xi) = (u_h(\xi), p_h(\xi), v_h(\xi), q_h(\xi))$ as a solution of system* (3.4) *which is homoclinic to* $(0,0,0,0)$ *and lies in the intersection $W^s(M_\varepsilon) \cap W^u(M_\varepsilon)$. Moreover,*

$$\begin{aligned} \|v_h(\xi) - v_{h,0}(\xi; u^*, 0)\|_\infty &= \mathcal{O}(\varepsilon), \\ \|q_h(\xi) - q_{h,0}(\xi; u^*, 0)\|_\infty &= \mathcal{O}(\varepsilon) \end{aligned} \tag{3.11}$$

for all $\xi \in \mathbb{R}$ and

$$\begin{aligned} \|u_h(R) - u_{h,0}(R - R^*)\|_\infty &= \mathcal{O}(\varepsilon), \\ \|p_h(R) - p_{h,0}(R - R^*)\|_\infty &= \mathcal{O}(\varepsilon) \end{aligned} \tag{3.12}$$

for all $R < 0$, while

$$\begin{aligned} \|u_h(R) - u_{h,0}(R + R^*)\|_\infty &= \mathcal{O}(\varepsilon), \\ \|p_h(R) - p_{h,0}(R + R^*)\|_\infty &= \mathcal{O}(\varepsilon) \end{aligned} \tag{3.13}$$

for all $R > 0$.

The orbit χ_h corresponds to a homoclinic solution (u_h, v_h) of system (1.6) *with $\delta = \varepsilon^2$, $\beta = T_1 = T_2 = 0$ and potential $W(u, v)$ as defined in* (3.1)*.*

Proof. The proof of the Theorem follows almost directly from the previous paragraphs and Fenichel Theory. The orbit $(v_h(\xi), q_h(\xi))$ is the perturbed equivalent of $(v_{h,0}, q_{h,0})$ with initial conditions $(u_0, p_0) = (u^*, 0)$. $p_0 = 0$ is where the intersection of $W^s(M_\varepsilon)$ and $W^u(M_\varepsilon)$ takes place, and $u_0 = u^*$ is where the orbit takes off into the fast field, and touches down once more.

For $-\infty < R < 0$, the orbit $u_h(R)$ is $\mathcal{O}(\varepsilon)$ close to a translation of the homoclinic $u_{h,0}$: it follows the homoclinic until the take-off point $R = -R^*$. The orbit $u_h(R)$ then continues to follow the homoclinic $u_{h,0}$ from the point $R = R^*$ onward until infinity.

For details on the precise estimates of equations (3.11), (3.12) and (3.13), the reader is referred to the results on slowly linear systems in [1]. □

Remark. Now that we have shown the existence of a homoclinic to the origin, it is time to come back to the singularity in this point. When we substitute the expressions for $u_{h,0}$ and $v_{h,0}$ into v^3/u we see that

$$\lim_{R \to \pm\infty} \frac{v_{h,0}(R)^3}{u_{h,0}(R)} = 0,$$

because $v_{h,0}^3$ goes to zero a lot faster than $u_{h,0}$. Thus we have no issues approaching the origin. The authors of [1] show that this can be extended to the $\mathcal{O}(\varepsilon)$ perturbed versions of these homoclinics, and thus to the 'total' homoclinic $\chi_h(\xi)$.

4 Constructing a stationary pulse solution for the thesis system

In the previous chapter we have shown that for the parameter choice $\beta = T_1 = T_2 = 0$ system (1.6) has a stationary pulse solution that is homoclinic to the origin. Now that we are a little bit familiar with the system and the mathematical techniques, we can try to construct a stationary pulse solution of the system for more general parameter values.

We let the interface curvature β be positive and make a 'simple' choice for the vector field T:

$$T = \begin{pmatrix} -v \\ u \end{pmatrix}.$$

Later on we will consider more general fields T. Note that $(T_1)_v \neq (T_2)_u$, meaning the vector field is indeed non-conservative.

The four-dimensional slow system now looks as follows:

$$\begin{aligned} u' =& \quad p \\ p' =& \quad \theta v + \tfrac{2}{3\theta u^2} v^3 + \alpha u - \gamma u^n - \tfrac{\varepsilon\beta}{R_0 + \varepsilon R} \cdot p - \varepsilon v \\ \varepsilon v' =& \quad q \\ \varepsilon q' =& \quad \theta u + v - \tfrac{2}{\theta u} v^2 - \tfrac{\varepsilon^2 \beta}{R_0 + \varepsilon R} \cdot q + \varepsilon u. \end{aligned} \tag{4.1}$$

And the corresponding fast sytem equals

$$\begin{aligned} \dot{u} =& \quad \varepsilon p \\ \dot{p} =& \quad \varepsilon \left(\theta v + \tfrac{2}{3\theta u^2} v^3 + \alpha u - \gamma u^n - \tfrac{\varepsilon\beta}{R_0 + \varepsilon R} \cdot p - \varepsilon v \right) \\ \dot{v} =& \quad q \\ \dot{q} =& \quad \theta u + v - \tfrac{2}{\theta u} v^2 - \tfrac{\varepsilon^2 \beta}{R_0 + \varepsilon R} \cdot q + \varepsilon u. \end{aligned} \tag{4.2}$$

4.1 Analyzing the fast system

We will follow the same approach as in paragraph 3.2 and start by setting $\varepsilon = 0$. All of the terms that are new in system (4.2) compared to system (3.4) are of $\mathcal{O}(\varepsilon)$ or higher, meaning the reduced fast system stays exactly the same. Thus the manifold M_0 defined in the previous paragraph is once more a normally hyperbolic invariant manifold of (4.2) with $\varepsilon = 0$ and the system has a family of homoclinics $(v_{h,0}, q_{h,0})$ for initial conditions (u_0, p_0) to this critical manifold.

Fenichel's first theorem now ensures the existence of a slow manifold M_ε that is $\mathcal{O}(\varepsilon)$ close to M_0 and that is locally invariant under the flow of the full system. However, where before the critical manifold M_0 was also locally invariant under the flow of the full system, we see that now this is not the case, because $\dot{q} \neq 0$ on M_0.

As we know from Fenichel Theory that M_ε is $\mathcal{O}(\varepsilon)$ away from M_0, we can find it explicitly. We define the slow manifold as

$$M_\varepsilon = \left\{ (u,p,v,q) \middle| u > 0, v = -\frac{1}{2}\theta u_0 + \varepsilon v_1, q = 0 + \varepsilon q_1 \right\}.$$

and substitute the equations for v and q into system (4.2). Because M_ε only sets restrictions on q and v we are solely interested in the equations for $\dot{v}$ and $\dot{q}$, which now are:

$$\begin{aligned}
\dot{v} &= \varepsilon q_1 \\
\dot{q} &= \theta u + \left(-\frac{1}{2}\theta u + \varepsilon v_1\right) - \frac{2}{\theta u}\left(-\frac{1}{2}\theta u + \varepsilon v_1\right)^2 + \varepsilon u + \mathcal{O}(\varepsilon^2) \\
&= 3\varepsilon v_1 + \varepsilon u + \mathcal{O}(\varepsilon^2).
\end{aligned}$$

The manifold M_ε needs to be locally invariant which means that we need to have $\dot{v} = \dot{q} = 0$, to leading order. This is the case when $q_1 = 0$ and $v_1 = -\frac{u}{3}$ so let $M_\varepsilon = \left\{(u,p,v,q)|u > 0,\ q = 0, v = -\frac{1}{2}\theta u - \frac{\varepsilon}{3}u\right\}$ is a manifold that is locally invariant under the flow of the complete system, to leading order.

As mentioned before for $\varepsilon = 0$ the manifolds $W^{s,u}(M_0)$ collide into a family of homoclinic orbits $(v_{h,0}, q_{h,0})$, and Fenichel's second theorem now ensures that there exist manifolds $W^{s,u}(M_\varepsilon)$ that are $\mathcal{O}(\varepsilon)$ close and diffeomorphic to this family of homoclinics. We are once more interested whether these manifolds intersect, the nature of these intersections and thus whether a homoclinic orbit to M_ε exists. Since we have some added terms in comparison with the previous chapter, we will need to calculate the change accumulated by the Hamiltonian function once more.

Since the unperturbed Hamiltonian function is the same as in the previous chapter, we still have that

$$\dot{H} = q\dot{q} - \dot{v}\left(\theta u + v - \frac{2}{\theta u}v^2\right) - \dot{u}\left(\theta v + \frac{2}{3\theta u^2}v^3\right).$$

But since we have some extra terms in the system of differential equations, substituting the values for $\dot{u}$, $\dot{v}$ and $\dot{q}$ gives a different expression compared to the previous chapter. Doing this substitution results in

$$\begin{aligned}
\dot{H} &= q\left(\theta u + v - \frac{2}{\theta u}v^2 - \frac{\varepsilon^2\beta}{R_0 + \varepsilon R}q + \varepsilon u\right) - q\left(\theta u + v - \frac{2}{\theta u}v^2\right) - \varepsilon p\left(\theta v + \frac{2}{3\theta u^2}v^3\right) \\
&= -\varepsilon\left(\frac{\varepsilon\beta}{R_0 + \varepsilon R}q^2 - u\cdot q + p\left(\theta v + \frac{2}{3\theta u^2}v^3\right)\right),
\end{aligned}$$

and if we again integrate over ξ and approximate (u,p,v,q) by (u_0, p_0, v_h, q_h) we can compute the distance between $W^s(M_\varepsilon)$ and $W^u(M_\varepsilon)$ in the hyperplane

$\{q = 0\}$ by

$$\Delta H = -\varepsilon \int_{-\infty}^{\infty} \underbrace{\frac{\varepsilon\beta}{R_0 + \varepsilon^2 \xi}(q_h)^2}_{(1)} - \underbrace{u_0 q_h}_{(2)} + \underbrace{p_0 \left(\theta v_h + \frac{2}{3\theta u_0^2} v_h^3\right)}_{(3)} \mathrm{d}\xi. \tag{4.3}$$

We are interested whether intersections between $W^s(M_\varepsilon)$ and $W^u(M_\varepsilon)$ exist and Melnikov Theory states this is the case for simple zeroes of ΔH. We can split the integral into three separate parts, as we have already indicated in equation (4.3), and calculate the integrals of each of these separately. Here we use that

$$q_{h,0} = \frac{dv_{h,0}}{d\xi} = \theta u_0 \frac{9\sqrt{3}}{4} \operatorname{sech}^2\left(\frac{\sqrt{3}}{2}\xi\right) \tanh\left(\frac{\sqrt{3}}{2}\xi\right).$$

Furthermore, we will expand the fraction $\frac{\beta}{R_0 + \varepsilon^2 \xi}$ as $\frac{\beta}{R_0}(1 + \mathcal{O}(\varepsilon))$ to show that the fraction is not dependent on ξ to leading order.

For the first two parts of (4.3) we use that $q_h h, 0$ is an odd function, and thus:

$$\begin{aligned}
\int_{-\infty}^{\infty} u_0 q_h \,\mathrm{d}\xi &= \tfrac{9\sqrt{3}}{4}\theta u_0^2 \int_{-\infty}^{\infty} \operatorname{sech}^2\left(\frac{\sqrt{3}}{2}\xi\right) \tanh\left(\frac{\sqrt{3}}{2}\xi\right) \\
&= \tfrac{9}{4}\theta u_0^2 \left[\operatorname{sech}^2\left(\tfrac{\sqrt{3}}{2}\xi\right)\right]_{-\infty}^{\infty} \\
&= 0
\end{aligned}$$

and

$$\begin{aligned}
\int_{-\infty}^{\infty} (q_h)^2 \,\mathrm{d}\xi &= \tfrac{243}{16}(\theta u_0)^2 \int_{-\infty}^{\infty} \operatorname{sech}^4\left(\frac{\sqrt{3}}{2}\xi\right) \tanh^2\left(\frac{\sqrt{3}}{2}\xi\right) \\
&= \tfrac{243}{16}(\theta u_0)^2 \cdot \tfrac{8\sqrt{3}}{45} = \tfrac{27\sqrt{3}}{10}(\theta u_0)^2,
\end{aligned}$$

to find that

$$\Delta H \approx -\frac{\varepsilon^2 \beta}{R_0} \frac{27\sqrt{3}}{10}(\theta u_0)^2 - \varepsilon p_0 \underbrace{\int_{-\infty}^{\infty} \theta v_h + \frac{2}{3\theta u_0^2} v_h^3 \,\mathrm{d}\xi}_{(3)}.$$

When we try to calculate the integral of (3) we run into a problem. Because $\lim_{\xi \to \pm\infty} v_h = -\frac{\theta u_0}{2}$ and the integral does not converge and we are not able to determine an initial p_0 for which $\Delta H = 0$. We will solve this by introducing a transformation of v, such that we will be able to evaluate the integral. The integral can be evaluated when the limit of v_h is not equal to $-\frac{\theta u_0}{2}$, but instead equals 0. To achieve this we will introduce the transformation $v \to \tilde{v} - \frac{1}{2}\theta u$, and we will expect that this transformation will result in a 'new' homoclinic $\tilde{v}_{h,0} = v_{h,0} + \frac{1}{2}\theta u_0 = \frac{9}{4}\theta u_0 \operatorname{sech}^2\left(\frac{\sqrt{3}}{2}\xi\right)$. This transformation is illustrated in

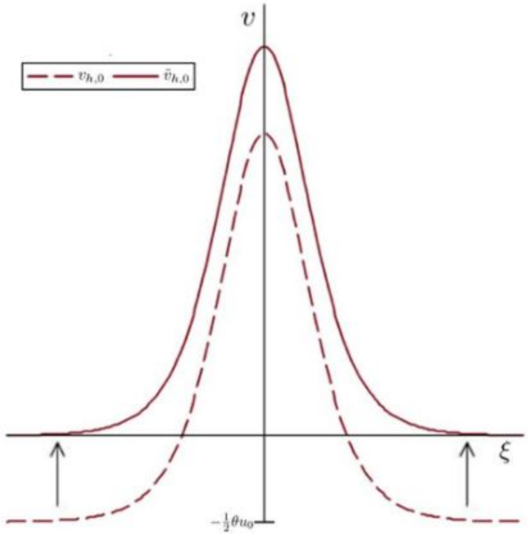

Figure 9: *An illustration of the transformation of $v_{h,0}$ to $\tilde{v}_{h,0}$.*

Figure 9.

In the next paragraph we will check whether this expectation is just and check what else changes about system (4.1) and our calculations after introducing $\tilde{v}$.

4.2 Introducing a transformed v

We will now introduce the transformation $v \to \tilde{v} - \frac{1}{2}\theta u$ in the fast system (4.2) to see if we get the desired homoclinic orbit with limits zero, and see what changes occur elsewhere. It is important to note that the transformation will also have an effect on the derivative of $\tilde{v}$, because of the u-term in the transformation. Hence we get the following transformed fast system:

$$\begin{aligned}
\dot{u} =& \quad \varepsilon p \\
\dot{p} =& \quad \varepsilon\left(\frac{3}{2}\theta\tilde{v} - \frac{\tilde{v}^2}{u} + \frac{2}{3\theta u^2}\tilde{v}^3 + \nu u - \gamma u^n - \frac{\varepsilon\beta}{R_0+\varepsilon R}\cdot p - \varepsilon(\tilde{v} - \frac{1}{2}\theta u)\right) \\
\dot{\tilde{v}} =& \quad \dot{v} + \frac{1}{2}\theta\dot{u} = q + \frac{\varepsilon}{2}\theta p \\
\dot{q} =& \quad 3\tilde{v} - \frac{2}{\theta u}\tilde{v}^2 - \frac{\varepsilon^2\beta}{R_0+\varepsilon R}\cdot q + \varepsilon u,
\end{aligned} \tag{4.4}$$

where we observe that the equation for $\dot{q}$ becomes simpler whereas the equation for $\dot{p}$ becomes a lot more complicated. We see that the system is still a Hamiltonian system for $\varepsilon = 0$, with Hamiltonian function $H(\tilde{v}, q) = \frac{1}{2}q^2 + \frac{2}{3\theta u}\tilde{v}^3 - \frac{3}{2}\tilde{v}^2$

and we can check that

$$\tilde{v}_{h,0}(\xi) = \frac{9}{4}\theta u_0 \operatorname{sech}^2\left(\frac{\sqrt{3}}{2}\xi\right)$$

and $\tilde{q}_{h,0}(\xi) = \frac{d\tilde{v}_{h,0}}{d\xi}$ is indeed a solution of $H(\tilde{v}, q) = 0$, as expected. Note that $\tilde{q}_{h,0}(\xi) = q_{h,0}(\xi)$ so we will use the latter notation henceforth.

So we found that the transformation $\tilde{v}$ indeed results in a more convenient homoclinic to do calculations with, but we must also take note of the fact that $M_0 = \left\{(u, p, \tilde{v}, q)|u > 0 \ q = 0, \tilde{v} = -\frac{1}{2}\theta u_0\right\}$ is now no longer a normally hyperbolic invariant manifold for the $\varepsilon = 0$ case. This occurs because we also translate the v-coordinate of the critical points of system (4.2) by $\frac{1}{2}\theta u_0$, hence setting $M_0 = \{(u, p, \tilde{v}, q)|u > 0, q = 0 = \tilde{v} = 0\}$ fixes this issue. As before, Fenichel's first theorem ensures the existence of a slow manifold M_ε, which we can find explicitly. We do this in the same manner as we did in paragraph 3.1, by setting $q = 0 + \varepsilon q_1$ and $\tilde{v} = 0 + \varepsilon\tilde{v}_1$ and substituting these into (4.4):

$$\begin{aligned}
\dot{\tilde{v}} &= \varepsilon q_1 + \frac{\varepsilon}{2}\theta p_0 \\
\dot{q} &= 3\varepsilon\tilde{v}_1 - \frac{2}{\theta u}(\varepsilon\tilde{v}_1)^2 - \frac{\varepsilon^2\beta}{R_0 + \varepsilon R} \cdot \varepsilon q_1 + \varepsilon u_0, \\
&= 3\varepsilon\tilde{v}_1 + \varepsilon u_0 + \mathcal{O}(\varepsilon^2).
\end{aligned}$$

The derivatives of $\tilde{v}$ and q become zero to leading order by setting $q_1 = -\frac{1}{2}\theta p_0$ and $\tilde{v}_1 = -\frac{1}{3}u_0$, which means that $M_\varepsilon = \left\{(u, p, \tilde{v}, q)|u > 0 \ q = -\frac{\varepsilon}{2}\theta p_0, \tilde{v} = -\frac{\varepsilon}{3}u_0\right\}$ is locally invariant under the flow of (4.4).

We have now shown that the introduction of $\tilde{v}$ gives us a homoclinic orbit over which we are able to integrate, while we are still able to apply Fenichel Theory. Thus we can now return to our calculation of ΔH and discover whether an intersection $W^s(M_\varepsilon) \cap W^u(M_\varepsilon)$ exists. But since we introduced a different v we will have to compute ΔH anew. We do this in the same manner as in previous paragraphs by computing the change in Hamiltonian H:

$$\begin{aligned}
\Delta H &= \int_{-\infty}^{\infty} q_{h,0}\dot{q} + \dot{\tilde{v}}\tilde{v}_{h,0}\left(\frac{2}{u_0}\tilde{v}_{h,0} - 3\right) - \dot{u}\frac{2}{3\theta u_0^2}\tilde{v}^3 \, \mathrm{d}\xi \\
&= -\varepsilon \int_{-\infty}^{\infty} \frac{\varepsilon\beta}{R_0 + \varepsilon^2\xi}(q_h)^2 - u_0 q_h - p_0\tilde{v}_h\left(\frac{2}{3\theta u_0^2}\tilde{v}_h^2 - \frac{\tilde{v}_h}{u} + \frac{3}{2}\theta\right) \mathrm{d}\xi.
\end{aligned}$$

This integral still consists of three parts and since q_h is the same as in the previous paragraph we already know that the first two integrals are equal to $-\frac{\varepsilon^2\beta}{R_0}\frac{27\sqrt{3}}{10}(\theta u_0)^2$. Thus we only need to compute the integral of the third part, and because of the transformation we introduced this is now a finite number.

We find that

$$\int_{-\infty}^{\infty} \tilde{v}_h \left(\frac{2}{3\theta u_0^2} \tilde{v}_h^2 - \frac{\tilde{v}_h}{u} + \frac{3}{2}\theta \right) \mathrm{d}\xi = \frac{27\sqrt{3}}{5}\theta^2 u_0. \tag{4.5}$$

Combining our results give us that

$$\Delta H = -\frac{27\sqrt{3}\varepsilon}{10R_0}\theta^2 u_0 \left(\varepsilon\beta u_0 + 2p_0 R_0\right),$$

which equals zero for $p_0 = -\frac{\varepsilon\beta u_0}{2R_0}$. Hence there still exists an intersection of $W^s(M_\varepsilon) \cap W^u(M_\varepsilon)$, and hence a homoclinic to the manifold M_ε. But where before this intersection was located at $p_0 = 0$ it is now located at $P(u) := -\frac{\varepsilon\beta u}{2R_0}$ which is a linear function in the (u, p)-plane.

4.3 The slow system on M_ε

We continue by studying the dynamics of the full system (4.4) on the slow manifold $M_\varepsilon = \left\{(u, p, \tilde{v}, q) | u > 0 \ q = -\frac{\varepsilon}{2}\theta p_0, \tilde{v} = -\frac{\varepsilon}{3}u_0\right\}$ to analyze how orbits in the slow field behave, and whether we can construct a stationary pulse solution to the origin $(u, p, v, q) = (0, 0, 0, 0)$.

Hence we substitute the q and $\tilde{v}$ equations that define M_ε into the transformed slow system, which is the slow equivalent of system (4.4):

$$\begin{aligned} u' =& \quad p \\ p' =& \quad \nu u - \gamma u^n - \varepsilon \frac{\beta}{R_0 + \varepsilon R} p + \mathcal{O}(\varepsilon^2) \\ \tilde{v}' =& \quad q' = 0 \end{aligned} \tag{4.6}$$

We observe that this system is an $\mathcal{O}(\varepsilon)$ perturbation of (3.9), the slow system on the M_ε we found in the previous chapter. Hence the system has the same homoclinic solution $(u_{h,0}, p_{h,0})$ on M_ε for $\varepsilon = 0$. However, this homoclinic orbit will not persist for other values of ε, due to the perturbation terms.

The system has the following Hamiltonian function for $\varepsilon = 0$:

$$H_2(u, p) = \frac{1}{2}p^2 - \frac{\nu}{2}u^2 + \frac{\gamma}{n+1}u^{n+1}.$$

Where before this function fully described the homoclinic orbit to the point $(u, p) = (0, 0)$, we now have the perturbations we need to take into account, meaning the homoclinic falls apart into a stable and unstable manifold to the origin. There is no easy way to explicitly determine these, so we will again use Melnikov Theory to describe the distance between these manifolds. Hence we compute the derivative of $H_2(u,p)$ with respect to R:

$$\begin{aligned}\frac{dH_2}{dR} &= pp' - u'(\nu u - \gamma u^n) \\ &= p\left(\nu u - \gamma u^n - \varepsilon\frac{\beta}{R_0+\varepsilon R}p\right) - p(\nu u - \gamma u^n) \\ &= -\varepsilon\frac{\beta}{R_0+\varepsilon R}p^2.\end{aligned}$$

We will now integrate this derivative evaluated at the homoclinic orbit of the unperturbed system, so at $(u_{h,0}, p_{h,0})$ as defined in paragraph 2.2, once more expanding the fraction $\frac{\beta}{R_0+\varepsilon R}$, which leads to

$$\Delta H_2 = -\varepsilon \int_{-\infty}^{\infty} \frac{\beta}{R_0} p_{h,0}^2 \,\mathrm{d}R,$$

to leading order.

When we applied Melnikov Theory in previous paragraphs, we were interested in finding simple zeroes of the Melnikov integral, because we wanted to find intersections of the stable and unstable manifold. In this case we see that there is no initial value involved that we can freely choose, as we could do before with p_0, so this integral has a fixed value unequal to zero. Hence the stable and unstable manifold will not intersect but will fall apart and wind around the center point $(u,p) = (\overline{u}, 0)$ at a fixed distance, crossing the u-axis. There are 2 possible situations, both displayed in Figure 10: Either the unstable manifold is the inner curve that winds around the center point and the stable manifold is the outer curve (Figure 10, left), or the stable manifold is the inner curve and the unstable manifold is the outer curve (Figure 10, right). Note that in the Figure, we exaggerated the distance ΔH_2 to make the picture more clear, since this distance is actually $\mathcal{O}(\varepsilon)$.

We are interested which of the situations occur in our system and can conclude this by the sign of the Melnikov Integral. The definition of the Melnikov Function is the value of the unstable manifold minus the value of the stable manifold, at a certain cross-section. Hence it is not a conventional non-negative distance function, since it will be less than zero when the stable manifolds intersects the cross-section 'further'. We can state this result in a lemma and use this to determine which curve represents the stable manifold:

Lemma 4.1. *Denote H_s as the u-coordinate of the intersection $W^s((0,0)) \cap \{p=0\}$ and H_u as the u-coordinate of the intersection $W^u((0,0)) \cap \{p=0\}$. If the Melnikov integral ΔH_2 is positive, then $H_s < H_u$, and vice versa.*

ΔH_2 is the integral over a quadratic function, multiplied by a constant the opposite sign of R_0. So if we assume that $R_0 > 0$, then ΔH_2 is negative. This assumption is in accordance with the biological background, since R_0 denoted

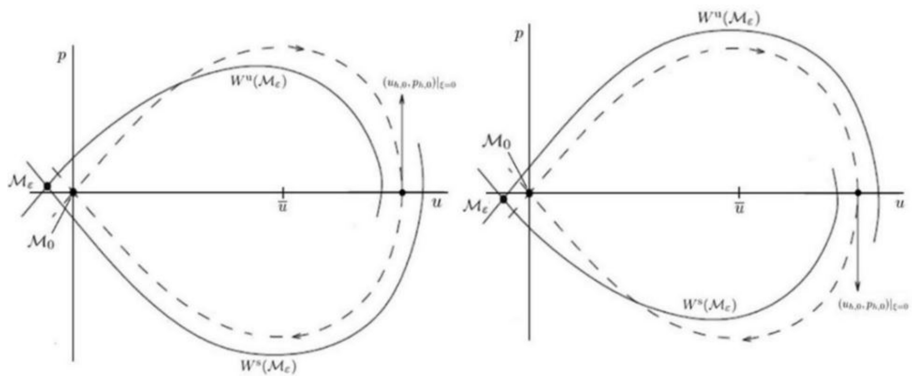

Figure 10: *The two possibilities for the breaking down of the homoclinic* $(u_{h,0}, p_{h,0})$ *(dashed) to the origin* $(0,0)$ *into an unstable and stable manifold that are a distance* ΔH_2 *from each other. The inner curve (*$W^u((0,0))$ *in the left figure and* $W^s((0,0))$ *in the right figure) wind around the equilibrium point* $\overline{u}$.

the radius of the single curvature interface.

Since H_2 is negative, the results stated above gives us that $W^u((0,0))$ is the inner curve and $W^s((0,0)$ is the outer curve, meaning in our system, the left situation in Figure 10 occurs.

Although we do not have explicit equations for the stable and unstable manifold of the slow system on M_ε, we do have a good notion of the location of these manifolds, and the distance between them, so we can continue our analysis by looking for the location of the jump through the fast field. Hence we are once more interested in the take-off and touchdown sets in M_ε. Once more we find these by computing the change accumulated by the p-coordinate during the excursion through the fast field. This gives

$$\begin{aligned}\Delta_\xi p \quad &= \varepsilon \int_{I_f} \frac{3}{2}\theta\tilde{v} - \frac{\tilde{v}^2}{u} + \frac{2}{3\theta u^2}\tilde{v}^3 + \nu u - \gamma u^n - \frac{\varepsilon\beta}{R_0 + \varepsilon R} \cdot p - \varepsilon(\tilde{v} - \frac{1}{2}\theta u)\,\mathrm{d}\xi \\ &\approx 2u_0\sqrt{\varepsilon}\left(\nu - \gamma u_0^{n-1}\right) + \varepsilon\frac{27\sqrt{3}}{5}\theta^2 u_0 + h.o.t.\end{aligned}$$

where we used the results from paragraph 3.2 and equation (4.5), meaning the change in p is not different from the unperturbed case to leading order. Also, because $\dot{u} = \varepsilon p$, we still have that $\Delta_\xi u = 0$ to leading order. But where with the unperturbed case we had that the transverse intersection of $W^s(M_\varepsilon) \cap W^u(M_\varepsilon)$ was located at $p = 0$, it is now located at $p = P(u)$ which means we have different take-off and touchdown curve.

Since the jump in p- direction is still symmetric around the transverse inter-

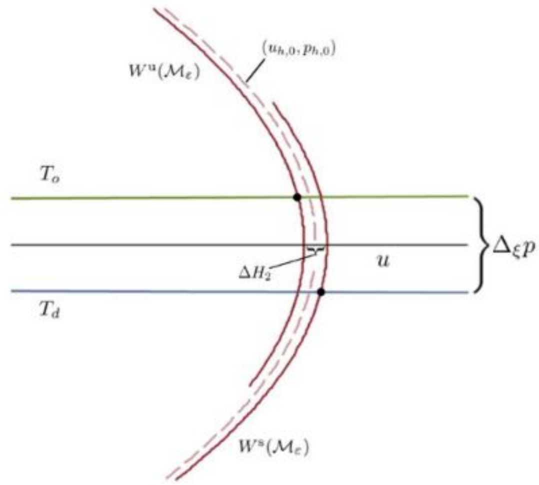

Figure 11: *Highly zoomed in figure showing the stable and unstable manifold to M_ε crossing the take-off and touchdown curve and the u-axis. Our desired take-off and touchdown point are indicated with dots, and the unperturbed homoclinic to M_0 is given as a dashed line. If the orbit in the fast field can 'jump' from the take-off point to the touchdown point, we know there exists a homoclinic orbit to the origin.*

section we get the following curves T_o and T_d:

$$\begin{aligned} T_o &:= \{(u,p,0,0) | p = -\frac{1}{2}\Delta_\xi p - \frac{\varepsilon\beta u}{2R_0}\}, \\ T_d &:= \{(u,p,0,0) | p = \ \ \frac{1}{2}\Delta_\xi p - \frac{\varepsilon\beta u}{2R_0}\}. \end{aligned}$$

A schematic picture of these curves and the perturbed stable and unstable manifold to M_ε are given in Figure 11. In this figure the take-off point is not directly above the touchdown point, implying the excursion through the fast field should accumulate some change Δu is well. Since we already determined that the change in u is zero to leading order, the figure makes us suspect that it is not possible to connect the unstable and stable manifold with the fast orbit. This would mean there does not exist a stationary pulse solution to the origin. In the next paragraph we confirm the suspicion aroused by Figure 11 by approximating the intersections of the take-off and touchdown curves with the unstable and stable manifold, respectively, and showing that these are not situated at the same u-coordinate.

4.4 The existence of a stationary pulse solution

Now we want to study whether there exists a stationary pulse solution of the general equations of this thesis, so whether there exists a homoclinic solution to

$(0, 0, 0, 0)$ of the system (4.1). If there exist points $(u_1, p_1) \in W^u(M_\varepsilon) \cap T_o$ and $(u_2, p_2) \in W^s(M_\varepsilon) \cap T_d$ with $u_1 = u_2$, we can use Fenichel Theory to conclude there exists a homoclinic to the origin. This homoclinic starts on the unstable manifold $W^u(M_\varepsilon)$, makes a excursion through the fast field starting close to the u-axis, after which it touches down to the manifold $W^s(M_\varepsilon)$ and goes back to the origin for $R \to \infty$.

In paragraph 3.5 we were immediately able to conclude that such points existed from the equation of the homoclinic solution and the fact that this solution was symmetrical around the u-axis, which was also the symmetry axis of the fast jump. Now we have lost this symmetry due to the fact that the stable and unstable manifold of M_ε do not coincide anymore, so we need to do some explicit calculations to discover if these points exist.

Thus we are now interested in the intersection of T_d and T_o with the stable and unstable manifolds of M_ε, respectively, but whereas we do have an explicit equation for the take-off and touchdown curves, we do not have that much information on the manifolds. We only know that they are $\mathcal{O}(\varepsilon)$ perturbations of the homoclinic solution $(u_{h,0}, p_{h,0})$ and that they are a distance ΔH_2 from each other, where the unstable manifold is the inner curve and the stable manifold the outer one. However, by taking a closer look at the Melnikov integral and what it is composed of we can find some additional information, in particular the exact distance between the manifolds and the homoclinic orbit. When we have this distance we may be able to give an approximate expression of the stable and unstable manifold, which will then make it possible for us to derive the intersections (u_1, p_1) and (u_2, p_2), up to a certain order.

As mentioned before the Melnikov Integral at a certain cross section is defined as the difference in value of the unstable manifold and the stable manifold, so at the cross section $\{p = 0\}$ this came down to $\Delta H_2 = H_u - H_s$, where H_u and H_s are the u-coordinates of the intersections of the unstable and stable manifold with the u-axis, respectively. Instead of focusing on the difference of these values we are now interested in these values separately, because if we can find an expression for H_u and H_s we can compute the distance of these points to the u-coordinate of the intersection H_{hom} of $(u_{h,0}, p_{h,0})$ with the u-axis.

We know that the manifold $W^u(M_\varepsilon)$ is a small perturbation of the homoclinic orbit, and that this perturbation is caused by the $\mathcal{O}(\varepsilon)$ terms. Thus at any point in 'time' $\hat{R}$, the location of the unstable manifold is equal to the location of the homoclinic orbit at that time, $(u_{h,0}(\hat{R}), p_{h,0}(\hat{R}))$, **plus** the change accumulated by the $\mathcal{O}(\varepsilon)$ terms in the period before $\hat{R}$. This gives us a way to calculate the value H_u, because we know due to symmetry that at $\hat{R} = 0$ the homoclinic orbit intersects the u-axis, and we defined this point as H_{hom}. Thus, $H_{hom} := u_{h,0}(0)$, and the above reasoning now leads to the following equation for H_u:

$$H_u = H_{hom} + \int_{-\infty}^{0} \frac{dH_2}{dR}(u_{h,0}, p_{h,0})\,\mathrm{d}R.$$

Similarly, the value of the stable manifold at a time $\hat{R}$ is equal to the value of the homoclinic at that time, **minus** the change the $\mathcal{O}(\varepsilon)$ terms will accumulate in the period after $\hat{R}$. Thus the points H_s can be computed by

$$H_s = H_{hom} - \int_{0}^{\infty} \frac{dH_2}{dR}(u_{h,0}, p_{h,0})\,\mathrm{d}R.$$

By subtracting H_s from H_u we can now check whether we find the same expression for ΔH_2 as given in previous paragraphs:

$$\begin{aligned}
\Delta H_2 = \quad & H_u - H_s \\
= \quad & \left(H_{hom} + \int_{-\infty}^{0} \frac{dH_2}{dR}(u_{h,0}, p_{h,0})\,\mathrm{d}R \right) - \left(H_{hom} - \int_{0}^{\infty} \frac{dH_2}{dR}(u_{h,0}, p_{h,0})\,\mathrm{d}R \right) \\
= \quad & \int_{-\infty}^{\infty} \frac{dH_2}{dR}(u_{h,0}, p_{h,0})\,\mathrm{d}R,
\end{aligned}$$

which is indeed the Melnikov Integral as we have defined it.

As mentioned above, H_{hom} is the value of the homoclinic orbit $u_{h,0}$ in $R = 0$ and we can thus give it explicitly:

$$H_{hom} = \left[\frac{\nu(n+1)}{2\gamma} \operatorname{sech}^2(0) \right]^{\frac{1}{n-1}} = \left(\frac{\nu(n+1)}{2\gamma} \right)^{\frac{1}{n-1}}.$$

Now recall that the derivative of H_2 to R evaluated at the homoclinic is equal to

$$\frac{dH_2}{dR}(u_{h,0}, p_{h,0}) = -\varepsilon \frac{\beta}{R_0 + \varepsilon R} p_{h,0}^2.$$

First we are interested in the value H_u so we will integrate this expression from $R = -\infty$ to 0. Here we will again expand the fraction $\frac{\beta}{R_0 + \varepsilon R}$ as $\frac{\beta}{R_0}(1 + \mathcal{O}(\varepsilon))$:

$$\int_{-\infty}^{0} \frac{dH_2}{dR}(u_{h,0}, p_{h,0})\,\mathrm{d}R \approx -\varepsilon \frac{\beta}{R_0} \int_{-\infty}^{0} p_{h,0}^2\,\mathrm{dR} := -\varepsilon \frac{\beta}{R_0} C_p.$$

Because it proves to be quite difficult to compute the above integral for a general value of n, we have just defined it as a constant C_p and note that this constant is positive and $\mathcal{O}(1)$. Hence we now get that:

$$H_u = H_{hom} + \int_{-\infty}^{0} \frac{dH_2}{dR}(u_{h,0}, p_{h,0})\,\mathrm{d}R = H_{hom} - \varepsilon \frac{\beta}{R_0} C_p.$$

In Appendix A.3 we have show that

$$p_{h,0}(R) = \frac{du_{h,0}}{dR} = -\sqrt{\nu}\tanh\left(\frac{(n-1)\sqrt{\nu}}{2}R\right)u_{h,0}$$

and because $u_{h,0}$ is an even function and the hyperbolic tangent an odd function, we have that $p_{h,0}$ is an odd function. Hence $p_{h,0}^2$ is an even function, meaning that

$$\int_0^\infty p_{h,0}^2 \,\mathrm{d}R = \int_{-\infty}^0 p_{h,0}^2 \,\mathrm{d}R = C_p$$

and thus $H_s = H_{hom} + \varepsilon\frac{\beta}{R_0}C_p$, and we check that indeed

$$\Delta H_2 = H_u - H_s = -\varepsilon\frac{\beta}{R_0}\int_{-\infty}^{\infty} p_{h,0}^2 \,\mathrm{d}R,$$

as we already found in paragraph 3.3.

Although we now know where the stable and unstable manifolds cross the u-axis, we still do not have exact expressions for these manifolds which makes it hard to compute the intersections with the take-off and touchdown curves. Hence we will approximate the stable and unstable manifolds by parabola in the (p,u)-plane, as well as the homoclinic orbit. We will approximate the homoclinic orbit by its second order Taylor approximation in the (p,u)-plane. Since the homoclinic equals zero in the point H_{hom}, we define the approximation $\hat{u}$ of $u_{h,0}$ close to $u = H_{hom}$ in the (p,u)-plane as follows:

$$\hat{u}(p) = H_{hom} - A\cdot p^2,$$

where A is a positive constant that follows from the Taylor series. Note that we are talking about parabola in the (p,u)-plane to avoid tedious notational issues with root-functions in the (u,p)-plane. We can now define approximations of the stable and unstable manifold similarly:

$$\begin{aligned}\hat{u}_s(p) &:= H_s - A\cdot p^2\\ \hat{u}_u(p) &:= H_u - A\cdot p^2,\end{aligned}$$

where the same A is used because the curves are parallel to leading order close to $u = H_{hom}$.

Because these functions are only approximations their intersections with the take-off and touchdown curve will also be approximations, but we hope these approximations will give us enough information to draw a conclusion about the existence of a homoclinic orbit to $(0,0,0,0)$. Hence we first calculate where the take-off curve T_o intersects $\hat{u}_u(p)$ by substituting the equation defining T_o

into the above equation for $\hat{u}_u(p)$. Now we define u_i as the u-coordinate of the intersection and find

$$\begin{aligned} u_i = \hat{u}_u(T_o) \quad &= H_u - A\left(-u_i\sqrt{\varepsilon}\left(\nu - \gamma u_i^{n-1}\right) - \frac{\varepsilon\beta u_i}{2R_0}\right)^2 \\ &= H_u - Au_i^2\varepsilon\left(\nu - \gamma u_i^{n-1} + \sqrt{\varepsilon}\frac{\beta}{2R_0}\right)^2 \\ &= H_u - Au_i^2\varepsilon\left((\nu - \gamma u_i^{n-1})^2 + \sqrt{\varepsilon}\frac{(\nu - \gamma u_i^{n-1})\beta}{R_0} + \mathcal{O}(\varepsilon)\right). \end{aligned}$$

Because we have found that $\Delta_\xi u = 0$ to leading order, the intersection of T_d and $\hat{u}_s(p)$ needs to lie exactly beneath the intersection of T_o and $\hat{u}_u(p)$, which means the intersection needs to have the same u-coordinate u_i. Thus we substitute the equation for T_d into $\hat{u}_s(p)$ and demand that the intersection point is again u_i, which gives us:

$$\begin{aligned} u_i = \hat{u}_s(T_d) \quad &= H_s - A\left(u_i\sqrt{\varepsilon}\left(\nu - \gamma u_i^{n-1}\right) - \frac{\varepsilon\beta u_i}{2R_0}\right)^2 \\ &= H_s - Au_i^2\varepsilon\left(\nu - \gamma u_i^{n-1} - \sqrt{\varepsilon}\frac{\beta}{2R_0}\right)^2 \\ &= H_s - Au_i^2\varepsilon\left((\nu - \gamma u_i^{n-1})^2 - \sqrt{\varepsilon}\frac{(\nu - \gamma u_i^{n-1})\beta}{R_0} + \mathcal{O}(\varepsilon)\right). \end{aligned}$$

If we now set these two results for u_i equal to each other and omit all terms of higher order than $\mathcal{O}(\varepsilon)$ we get as a strict demand for the existence of a jump from the unstable to the stable manifold that

$$H_u - Au_i^2\varepsilon(\nu - \gamma u_i^{n-1})^2 = H_s - Au_i^2\varepsilon(\nu - \gamma u_i^{n-1})^2,$$

and hence that

$$H_u - H_s = \Delta H_2 = 0.$$

Hence we can only construct a homoclinic to the critical point $(0,0,0,0)$ if the stable and unstable manifold coincide, which we know is not the case when $\beta \neq 0$. This means it is impossible to have a stationary pulse solution for our general problem with the current assumptions.

Theorem 4.1 (Existence of a stationary pulse solution)**.** *Let $\varepsilon > 0$ be sufficiently small. Then, for all values of the parameters $\theta > 0$, $\gamma > 0$, $\alpha > \frac{7}{12}\theta^2$ and $n > 1$, there exists a unique orbit $\gamma_h(\xi) = (u_h(\xi), p_h(\xi), v_h(\xi), q_h(\xi))$ as a solution of system* (4.2) *which is homoclinic to* $(0,0,0,0)$ *and lies in the intersection* $W^s(M_\varepsilon) \cap W^u(M_\varepsilon)$ ***if and only if*** $\beta = 0$.

Proof. Let $\beta = 0$ in system (4.1). Then $\Delta H_2 = 0$ and the stable and unstable manifold of M_ε coincide into a homoclinic orbit. Also, setting $\beta = 0$ in the take-off and touchdown curves makes these the same as in chapter 3. Thus with the same arguments used in the proof of theorem 4.1, we can now construct an orbit χ_h that is homoclinic to the origin.

If $\beta \neq 0$, then $\Delta H_2 \neq 0$ and the stable and unstable manifold of the origin on M_ε do not coincide but are separated. In this case there is no orbit in $W^s(M_\varepsilon) \cap W^u(M_\varepsilon)$ bi-asymptotic to M_ε, meaning a homoclinic to the point $(0, 0, 0, 0)$ does not exist. □

With this theorem we can conclude that the inclusion of a curvature term, represented by parameter β, dismisses the existence of a homoclinic orbit to the origin, and thus to the existence of a stationary pulse solution.

This result concludes the main work of this thesis, but what stands out in theorem 4.1 is that the addition of the vector field T did not have any effect on the existence of a stationary pulse solution. The choice $T = (-v, u)^T$ resulted in a different, perturbed slow manifold compared to the $\vec{T} = 0$ case, but on this slow manifold and in the Hamiltonian functions, the terms of T dropped out. In the next paragraph we will study whether this holds for a general vector field T and hence if the vector has any real influence on the system.

4.5 Generalizing the vector field T

We concluded that the choice of the vector field T we made in the previous section did not have any real effect on the existence of a stationary pulse, because the terms dropped out to leading order. We are now interested whether this is only the case for our particular choice of the vector field, or holds for a more general T. We will thus analyze system (1.6) for a general T and research what influence this field has on the existence of a stationary pulse solution.

Because the vector field T is multiplied by a factor ε we do not need to consider it in the analysis when $\varepsilon = 0$, which means the critical manifold M_0 and Hamiltonian function H are not influenced by T and are equal to the ones defined in paragraph 3.3. However, the vector field T does influence the slow manifold M_ε when we set $\varepsilon \neq 0$. Finding this slow manifold corresponds to setting the derivatives of $\tilde{v}$ and q to zero and solving for $\tilde{v}$ and q, analogous to paragraph 4.2, meaning we need to solve:

$$\begin{aligned} \varepsilon q_1 + \frac{\varepsilon}{2}\theta p_0 = &\quad 0 \\ 3\varepsilon \tilde{v}_1 + \varepsilon T_2 + \mathcal{O}(\varepsilon^2) = &\quad 0. \end{aligned}$$

Note that we are still using the transformed variable $\tilde{v} = v + \frac{1}{2}\theta u$ as introduced in paragraph 4.2.

The upper equation leads to $q_1 = \frac{1}{2}\theta p_0$, which we also saw in previous paragraphs. The lower equation is less simple to solve, since T_2 can depend on $\tilde{v}$ as well. Depending on the choice of T_2, there can thus be none, one or multiple $\tilde{v}$ solving this equation. To solve this issue we narrow the collection of possible vector fields T a little by demanding T_2 does not depend on $\tilde{v}$, meaning the lower equation is solved by $\tilde{v}_1 = -\frac{1}{3}T_2$, to leading order. Thus we now have a slow manifold

$$M_\varepsilon := \left\{(u, p, \tilde{v}, q) | q = -\frac{\varepsilon}{2}\theta p_0, \tilde{v} = -\frac{\varepsilon}{3}T_2(u_0)\right\}.$$

Although the Hamiltonian function is the same as in the previous chapters, the vector T possibly has a contribution to ΔH, making it wise to reconstruct this value. We have

$$\Delta H \quad = -\varepsilon \int_{-\infty}^{\infty} \frac{\varepsilon\beta}{R_0 + \varepsilon^2\xi}(q_h)^2 - T_2(u_0)q_h - p_0\tilde{v}_h \left(\frac{2}{3\theta u_0^2}\tilde{v}_h^2 - \frac{\tilde{v}_h}{u} + \frac{3}{2}\theta\right) \mathrm{d}\xi,$$

where the only relevant term for the research in this paragraph is the integral of $T_2 q_h$. Since T_2 does not depend on $\tilde{v}$, it is constant in the fast field. Furthermore, q_h is an odd function, which means the integral of $T_2 q_h$ equals zero. Thus, the vector field T does not have any influence on the value of ΔH.

If we now substitute the manifold M_ε into the slow system, we get

$$\begin{aligned} u' &= p \\ p' &= \nu u - \gamma u^n - \varepsilon\left(\tfrac{\beta}{R_0+\varepsilon R}p + \tfrac{\theta}{2}T_2 - T_1\right). \end{aligned}$$

For $\varepsilon = 0$ this system has the same Hamiltonian function H_2 as in section, and if we now take the derivative of this function with respect to R we get that

$$\frac{dH_2}{dR} = -\varepsilon p\left(\frac{\beta}{R_0 + \varepsilon R}p + \frac{\theta}{2}T_2 - T_1\right).$$

Since we are interested in the contribution T has to the value of ΔH_2 we are interested in the value of

$$\int_{-\infty}^{\infty} p_{h,0}\left(\frac{\theta}{2}T_2(u_{h,0}) - T_1(u_{h,0}, \tilde{v})\right) \mathrm{d}R.$$

Recall that in the slow system the variable v stays approximately constant, which would mean that $T_{1,2}$ both only depend on the variable u. Thus we can define $T^*(u) := \frac{\theta}{2}T_2(u) - T_1(u, \tilde{v}_{h,0})$, where $\tilde{v}_{h,0} = v_{h,0} + \frac{1}{2}\theta u$, which leaves us with calculating

$$\int_{-\infty}^{\infty} p_{h,0}T^*(u_{h,0})\,\mathrm{d}R.$$

Lemma 4.2. *For any $a \in \mathbb{R}$, $n \in \mathbb{N}$*

$$\int_{-\infty}^{\infty} \operatorname{sech}^n(ax)\tanh(ax)\,\mathrm{d}x = 0,$$

and from this it follows that

$$\int_{-\infty}^{\infty} p_{h,0}T^*(u_{h,0})\,\mathrm{d}R = 0.$$

Proof. For any $a \in \mathbb{R}$ the function $\tanh(ax)$ is odd while the function $\operatorname{sech}^n(ax)$ is even for any $n \in \mathbb{N}$. Hence their product is an odd function which immediately leads to

$$\int_{-\infty}^{\infty} \operatorname{sech}^n(ax)\tanh(ax)\,\mathrm{d}x = 0,$$

Now, recall that $p_{h,0}$ is the product of a hyperbolic secant and tangent, whereas $u_{h,0}$ is a hyperbolic tangent. Since T^* is a polynomial in u, the function $p_{h,0}T^*(u_{h,0})$ is a sum of products of a hyperbolic tangent and a power of a hyperbolic secant, meaning each separate part integrates to zero. Thus,

$$\int_{-\infty}^{\infty} p_{h,0}T^*(u_{h,0})\,\mathrm{d}R = 0.$$

□

The above Lemma thus shows us that the vector T, under the conditions we have defined, has no contribution to the value of ΔH_2.

In this thesis we have calculated $\Delta_\xi p$ by integrating p_ξ over an interval I_f. The terms of this calculation that involve the vector T are

$$\varepsilon^2 \int_{-\frac{1}{\sqrt{\varepsilon}}}^{\frac{1}{\sqrt{\varepsilon}}} \frac{\theta}{2}T_2 - T_1\,\mathrm{d}\xi,$$

and because the integrand is $\mathcal{O}(1)$, the above term is $\mathcal{O}(\varepsilon^{3/2})$. This is a higher order term which we will leave out of consideration when using $\Delta_\xi p$, meaning the vector T has no relevant contribution to $\Delta_\xi p$.

We can conclude that for a certain class of vector fields T, the field does not have any contribution to the values of $\Delta H, \Delta H_2$ and $\Delta_\xi p$. We can now state the following theorem on T:

Theorem 4.2. *Let $T = (T_1(u,v), T_2(u))^T$ be a non-conservative vector field, where T_1 is a polynomial in u and v and T_2 a polynomial in u. Then the vector field T does not have any influence on the existence of a stationary pulse solution.*

Proof. We have shown that a vector field T with properties as in Theorem 4.2 does not have any contribution to the values of $\Delta H, \Delta H_2$ and $\Delta_\xi p$. Since these values are the only relevant values for the existence of a stationary pulse solution, we can conclude that T does not influence this existence. □

Remark. We have seen that the vector field T **does** have influence on the collection M_ε, meaning it would not be justified to omit it from the system entirely.

5 Conclusion

Although the model used in this thesis has a solid biological foundation based on various experimental observations and results, it was never the goal of this thesis to reach biologically relevant results. Most of the assumptions made are biologically not realistic, and some were made purely to make mathematical analysis possible. This is why I will start this conclusion by discussing the mathematical results, and come back later to the biological interpretation and discussion.

Putting aside the biological interpretation, the goal of this thesis was finding a specific type of solution, a homoclinic orbit to the origin, of a singularly perturbed four-dimensional system of differential equations. Anything four-dimensional somewhat supersedes the imagination of us three-dimensional creatures, which made visually interpreting this solution the first challenge of this thesis. What greatly helped to me were visualizations of homoclinic solutions of three-dimensional systems, which is one of the reasons I added the example in paragraph 2.3 to this thesis.

The approach I have used is a great example of how old(er) theory can be used together with new(er) results, to solve a system with a complete unrelated background. The results on singularly perturbed systems posed by Fenichel and described by Jones in [5], in combination with Frits Veerman's PhD Thesis [9] on a four-dimensional system similar to mine, made up a mathematical basis from which I could start my research and fall back on whenever necessary.

In this thesis, I have shown the existence of a stationary pulse solution of the four-dimensional system under consideration, system (2.5), where the bilayer has no curvature, corresponding to a factor $\beta = 0$ (see Figure 3). We were even able to show that this result holds for a very broad class of vector fields T. This was something I did not expect from the outset.

However, the assumption that $\beta = 0$ was made originally to explore the system, and our intention was to continue the analysis for a general value of this parameter. For a general value of $\beta > 0$, we were able to show that it is not possible to construct a stationary pulse solution, implying a configuration as in Figure 1 does not exist as a steady state of the system. Since these configurations have been found experimentally this implication is untrue, which in turn implies the system does not model the biological setting correctly.

To apply our mathematical techniques to the system, we made the crude assumption that the dominant terms of (1.1) completely described the dynamics of the model, as mentioned in the introduction. With this, we reduced the 'real' problem from solving an 8-dimensional system of differential equations to a 4-dimensional system, making the analysis better possible. It could well be that with this assumption, we effectively made the construction of a stationary pulse solution impossible. This leads to some interesting follow-up questions. It might be that the form of W as posed in [8] is necessary for the analysis of the two-component FCH. Also, it could be that introducing the curvature into the reduced 4-dimensional system was not the right plan of action, and this curvature should be incorporated only when analyzing the full 8-dimensional system.

Although this thesis did not lead to a stationary pulse solution of the multi-component functionalized Cahn-Hilliard Free Energy, I am convinced there is a lot more knowledge to be gained regarding this subject. There has been a lot of research regarding the FCH as a model for amphiphilic polymer configurations in a bulk solvent, the analysis of the multi-component case is still in its early years. This thesis and its conclusions on the presence of a curvature factor β, together with the new insights on the function W in [8], could form the basis to new research on this topic which may lead to positive results on the existence of stationary pulse solutions of the equation.

6 Appendix A: Calculations

The derivative of $y = \operatorname{sech}^b(x)$ We can calculate the derivative of $y(x) = \operatorname{sech}^b(x)$ by using the chain rule, after which we use some rules about hyperbolic function to get back an equation in terms of y:

$$\begin{aligned}\frac{dy}{dx} &= b \operatorname{sech}^{b-1}(x) \cdot (-\operatorname{sech}(x)\tanh(x)) \\ &= -b \operatorname{sech}^b(x)\tanh(x) \\ &= -by(x)\tanh(x).\end{aligned}$$

Now we use that $\tanh^2(x) + \operatorname{sech}^2(x) = 1$ to get $\tanh(x) = \sqrt{1 - \operatorname{sech}^2(x)} = \sqrt{1 - \left(\operatorname{sech}^b\right)^{\frac{2}{b}}} = \sqrt{1 - y(x)^{\frac{2}{b}}}$. Substituting this gives us

$$\frac{dy}{dx} = -by(x)\sqrt{1 - y(x)^{\frac{2}{b}}}.$$

Calculation of the constant c in $v_{h,0}(\xi)$ Let the function $v_{h,0}(\xi)$ be as follows

$$v_{h,0}(\xi) = \theta u_0 \left(\frac{9}{4}\operatorname{sech}^2(c\xi) - \frac{1}{2}\right)$$

with c an unknown non-zero constant and assume that $v_{h,0}$ solves the differential equation

$$\left(\frac{dv}{d\xi}\right)^2 = 2\theta u_0 v + v^2 - \frac{4}{3\theta u_0}v^3 + \frac{7}{12}(\theta u_0)^2. \tag{6.1}$$

We first calculate the derivative of $v_{h,0}$ and square it:

$$\begin{aligned}\left(\frac{dv_{h,0}}{d\xi}\right)^2 &= \left(\frac{9}{2}c\theta u_0 \operatorname{sech}^2(c\xi)\tanh(c\xi)\right)^2 \\ &= \frac{81}{4}c^2(\theta u_0)^2 \operatorname{sech}^4(c\xi)\tanh^2(c\xi) \\ &= \frac{81}{4}c^2(\theta u_0)^2 \operatorname{sech}^4(c\xi)(1 - \operatorname{sech}^2(c\xi)).\end{aligned}$$

We also have

$$\begin{aligned}(v_{h,0})^2 &= (\theta u_0)^2 \left(\frac{81}{16}\operatorname{sech}^4(c\xi) - \frac{9}{4}\operatorname{sech}^2(c\xi) + \frac{1}{4}\right) \\ (v_{h,0})^3 &= (\theta u_0)^3 \left(\frac{729}{64}\operatorname{sech}^6(c\xi) - \frac{243}{32}\operatorname{sech}^4(c\xi) + \frac{27}{16}\operatorname{sech}^2(c\xi) - \frac{1}{8}\right).\end{aligned}$$

Now we want to compute the right-hand side of (6.1) in $v_{h,0}(\xi)$ and do this by collecting terms of the same power of $\operatorname{sech}(c\xi)$. This results in:

$$\begin{aligned}
O(1): &\quad (\theta u_0)^2\left(-1+\tfrac{1}{4}+\tfrac{1}{6}+\tfrac{7}{12}\right)=0\\
O(\operatorname{sech}^2(c\xi)): &\quad (\theta u_0)^2\left(\tfrac{9}{2}-\tfrac{9}{4}-\tfrac{9}{4}\right)=0\\
O(\operatorname{sech}^4(c\xi)): &\quad (\theta u_0)^2\left(\tfrac{81}{16}+\tfrac{81}{8}\right)=\tfrac{243}{16}(\theta u_0)^2\\
O(\operatorname{sech}^6(c\xi)): &\quad -\tfrac{243}{16}(\theta u_0)^2.
\end{aligned}$$

This means that

$$2\theta u_0 v_{h,0}+(v_{h,0})^2-\frac{4}{3\theta u_0}(v_{h,0})^3+\frac{7}{12}(\theta u_0)^2=\frac{243}{16}(\theta u_0)^2\operatorname{sech}^4(c\xi)(1-\operatorname{sech}^2(c\xi)),$$

which is equal to $\left(\frac{dv_{h,0}}{d\xi}\right)^2$ for $c=\pm\frac{\sqrt{3}}{2}$.

Correctness of $u_{h,0}$ We claim that the homoclinic

$$u_{h,0}(R)=\left[\frac{\nu(n+1)}{2\gamma}\operatorname{sech}^2\left(\frac{1}{2}(n-1)\sqrt{\nu}R\right)\right]^{\frac{1}{n-1}}, \tag{6.2}$$

solves the differential equation

$$\left(\frac{du}{dR}\right)^2=u^2\left(\nu-\frac{2\gamma}{n+1}u^{n-1}\right). \tag{6.3}$$

First we compute the derivative of $u_{h,0}$ with respect to R

$$\begin{aligned}
\left(\frac{du_{h,0}}{dR}\right) &= \frac{1}{n-1}\left[\frac{\nu(n+1)}{2\gamma}\operatorname{sech}^2\left(\frac{1}{2}(n-1)\sqrt{\nu}R\right)\right]^{\frac{1}{n-1}-1}\cdot\\
&\quad\left(-2\frac{\nu(n+1)}{2\gamma}\operatorname{sech}^2\left(\frac{1}{2}(n-1)\sqrt{\nu}R\right)\tanh\left(\frac{1}{2}(n-1)\sqrt{\nu}R\right)\frac{n-1}{2}\sqrt{\nu}\right)\\
&= -\sqrt{\nu}\tanh\left(\frac{1}{2}(n-1)\sqrt{\nu}R\right)\left[\frac{\nu(n+1)}{2\gamma}\operatorname{sech}^2\left(\frac{1}{2}(n-1)\sqrt{\nu}R\right)\right]^{\frac{1}{n-1}}\\
&= -\sqrt{\nu}\tanh\left(\frac{1}{2}(n-1)\sqrt{\nu}R\right)u_{h,0}.
\end{aligned}$$

If we square this result we see that (6.3) holds if $u_{h,0}=0$ or if

$$\nu\tanh^2\left(\frac{1}{2}(n-1)\sqrt{\nu}R\right)=\nu-\frac{2\gamma}{n+1}(u_{h,0})^{n-1}. \tag{6.4}$$

From equation (6.2) we can compute $(u_{h,0})^{n-1}$ and get

$$\begin{aligned}
(u_{h,0})^{n-1} &= \frac{\nu(n+1)}{2\gamma}\operatorname{sech}^2\left(\frac{1}{2}(n-1)\sqrt{\nu}R\right)\\
&= \frac{\nu(n+1)}{2\gamma}\left(1-\tanh^2\left(\frac{1}{2}(n-1)\sqrt{\nu}R\right)\right).
\end{aligned}$$

This means the right-hand side of (6.4) can be rewritten to

$$\begin{aligned}\nu-\frac{2\gamma}{n+1}(u_{h,0})^{n-1} &= \nu-\frac{2\gamma}{n+1}\cdot\frac{\nu(n+1)}{2\gamma}\left(1-\tanh^2\left(\frac{1}{2}(n-1)\sqrt{\nu}R\right)\right)\\ &= \nu-\nu\left(1-\tanh^2\left(\frac{1}{2}(n-1)\sqrt{\nu}R\right)\right)\\ &= \nu\tanh^2\left(\frac{1}{2}(n-1)\sqrt{\nu}R\right),\end{aligned}$$

showing that $u_{h,0}$ indeed solves (6.3).

Calculation of $\Delta_\xi p$ We want to calculate

$$\Delta_\xi p = \int_{I_f}\dot{p}\,\mathrm{d}\xi = \varepsilon\int_{I_f}\underbrace{\theta v}_{(1)}+\underbrace{\frac{2}{3\theta u^2}v^3}_{(2)}+\underbrace{\alpha u-\gamma u^n}_{(3)}\,\mathrm{d}\xi, \tag{6.5}$$

where we will split the integral into three smaller parts (1), (2) and (3) and calculate these parts separately. Because of our choice of interval we can take $v = v_{h,0}$ and $u = u_0$, so for the first part (1) we get:

$$\begin{aligned}\int_{I_f}\theta v_{h,0}\,\mathrm{d}\xi &= \int_{I_f}\theta^2 u_0\left(\frac{9}{4}\operatorname{sech}^2\left(\frac{\sqrt{3}}{2}\xi\right)-\frac{1}{2}\right)\mathrm{d}\xi\\ &= \theta^2 u_0\left[\tfrac{3\sqrt{3}}{2}\tanh\left(\tfrac{\sqrt{3}}{2}\xi\right)-\tfrac{\xi}{2}\right]_{-\frac{1}{\sqrt{\varepsilon}}}^{\frac{1}{\sqrt{\varepsilon}}}\\ &= \theta^2 u_0\left(-\tfrac{1}{\sqrt{\varepsilon}}+\frac{3\sqrt{3}\left(\mathrm{e}^{\sqrt{\frac{3}{\varepsilon}}}-1\right)}{\mathrm{e}^{\sqrt{\frac{3}{\varepsilon}}}+1}\right)\\ &\approx \theta^2 u_0\left(-\tfrac{1}{\sqrt{\varepsilon}}+3\sqrt{3}\right),\end{aligned}$$

where we used that $\varepsilon \ll 1$ and that

$$\lim_{x\to\infty}\frac{\mathrm{e}^x-1}{\mathrm{e}^x+1}=1.$$

We continue with calculating (2), where we use the expression for $(v_{h,0})^3$ computed on the previous page. Thus

$$\begin{aligned}\int_{I_f}\frac{2}{3\theta u^2}(v_{h,0})^3\,\mathrm{d}\xi &= \frac{2}{3}\theta^2 u_0\int_{I_f}\frac{729}{64}\operatorname{sech}^6\left(\frac{\sqrt{3}}{2}\xi\right)-\frac{243}{32}\operatorname{sech}^4\left(\frac{\sqrt{3}}{2}\xi\right)+\frac{27}{16}\operatorname{sech}^2\left(\frac{\sqrt{3}}{2}\xi\right)-\frac{1}{8}\,\mathrm{d}\xi\\ &\approx \theta^2 u_0\left(\frac{12\sqrt{3}}{5}-\frac{1}{6\sqrt{\varepsilon}}\right).\end{aligned}$$

Lastly we calculate expression (3), which is just a constant in the fast field so

$$\int_{I_f}\alpha u-\gamma u^n\,\mathrm{d}\xi = \frac{2}{\sqrt{\varepsilon}}\left(\alpha u_0-\gamma u_0^n\right).$$

Combining all this gives us that

$$
\begin{aligned}
\Delta_\xi p &= \varepsilon\left(\theta^2 u_0\left(-\frac{1}{\sqrt{\varepsilon}}+3\sqrt{3}\right)+\theta^2 u_0\left(\frac{12\sqrt{3}}{5}-\frac{1}{6\sqrt{\varepsilon}}\right)+\frac{2}{\sqrt{\varepsilon}}\left(\alpha u_0-\gamma u_0^n\right)\right)\\
&= \varepsilon\left(\frac{27\sqrt{3}}{5}\theta^2 u_0+\frac{2}{\sqrt{\varepsilon}}\left(\alpha u_0-\gamma u_0^n-\frac{7}{12}\theta^2 u_0\right)\right)\\
&= 2\sqrt{\varepsilon}u_0\left(\nu-\gamma u_0^{n-1}\right)+\varepsilon\frac{27\sqrt{3}}{5}\theta^2 u_0.
\end{aligned}
$$

References

[1] A. Doelman, R. Gardner, T. Kaper, *Large Stable Pulse Solutions in Reaction-diffusion Equations*, Indiana University Mathematics Journal, Vol. 50, No. 1 (2001).

[2] A. Doelman, G. Hayrapetyan, K. Promislow and B. Wetton, *Meander and pearling of functionalized of single-curvature bilayer interfaces in the functionalized Cahn-Hilliard equation*, SIAM Journal on Mathematical Analysis, Vol. 46 (2014).

[3] G. Hek, *Bifurcations of homoclinic orbits in singularly perturbed flows*, Phd Thesis, University Utrecht (2000).

[4] G. Hek, *Geometric Singular Perturbation Theory in biological practice*, Journal of Mathematical Biology, Vol. 60 (2010).

[5] C. Jones, *Geometric Singular Perturbation Theory*, Lecture Notes in Mathematics, Vol. 1609 (1994).

[6] T. Kaper, *An Introduction to Geometric Methods and Dynamical Systems Theory for Singular Perturbation Problems*, Proceedings of Symposia in Applied Mathematics, Volume 56 (1999).

[7] N. Kraitzman and K. Promislow, *An Overview of Network Bifurcations in the Functionalized Cahn-Hilliard Free Energy* in *Mathematics of Energy and Climate Change*, Springer (2015).

[8] K. Promislow and Q. Wu, *Existence, Bifurcation, and Geometric Evolution of Quasi-Bilayers in the Multicomponent Functionalized Cahn-Hilliard Equation*, Article submitted for publication (2016).

[9] F. Veerman and Arjen Doelman, *Pulses in a Gierer-Meinhardt Equation with a Slow Nonlinearity*, SIAM Journal of Applied Dynamical Systems, Vol 12 (2013).